05

III

# SEA ICE STUDIES IN THE SPITSBERGEN - GREENLAND AREA

Investigation No 28 540

E77-10206
CR-155776

Final Report

from


Torgny E. Vinje

Norwegian Polar Research Institute

Post office box 158

1330 Oslo Lufthavn

Norway




August 1977


(E77-10206) SEA ICE STUDIES IN THE SPITSBERGEN-GREENLAND AREA Final Report (Norsk Polarinstitutt) 47 p HC A03/MF A01 CSCL 08L

N77-31561

Unclas

G3/43 00206



Sponsoring organization: The Royal Norwegian Council for Scientific and Industrial Research (NTNF), Wdm. Thranesgt. 98, OSLO 1, Norway

# N O T I C E

THIS DOCUMENT HAS BEEN REPRODUCED FROM THE BEST COPY FURNISHED US BY THE SPONSORING AGENCY. ALTHOUGH IT IS RECOGNIZED THAT CERTAIN PORTIONS ARE ILLEGIBLE, IT IS BEING RELEASED IN THE INTEREST OF MAKING AVAILABLE AS MUCH INFORMATION AS POSSIBLE.

Table of Contents





List of Figures

## INTRODUCTION

The overall objective of this investigation is to utilize Landsat data to study sea ice in general and in the Spitsbergen-Fram Strait area in particular and to compare the usefulness of Landsat and weather satellite data (NOAA-2, ESSA-3, etc.) for studying sea ice. The specific objectives are as follows:

1. To develop a technique for forecasting changes in the position and concentration of sea ice in the Spitsbergen-Fram Strait area due to the influence of weather (primarily wind) and ocean currents.

2. To determine the physical characteristics of sea ice and ice boundaries, including statistical data on the dimensions and forms of ice floes.

3. To determine ice drift velocities in the East Greenland Current, and thereby obtain an estimate of the outflow of ice from the Arctic Basin.



This investigation has run over a period of two years, 1975 and 1976. During the first year 48 scenes were received. The material was, however, unsystematically collected and little information on drift of sea ice was obtained. During 1976, on the other hand, a great number of imageries were received, altogether 468, and numerous ice drift estimations have been obtained, particularely for April and May, which as usual were the most cloudless months. The weather during the period June - September was characterized by an extraordinary high cyclonic activity in the Svalbard area and because of hig cloudiness relatively few imageries have been obtained for this period.

## TECHNIQUES

MSS 7 of all the negatives received have been copied in BW at 1:1 mill scale. MSS 4 has been used for several scenes for a closer study of special features on bare land and open sea.

From BW MSS 7 a great number of ice floes have been traced from day to day. Where land can be seen on the imageries, correct position can be determined, otherwise the drift estimations are influenced by position errors 1-2 km, which are found in the Landsat positioning system (NYE 1974). For velocities greater than 10cm $S^{-1}$ the maximum error will decrease to less than 4% after a period of 5 days.

The frequency distribution of the size of the floes have been determined from BW (1:500 000 scale) by a semiautomatic planimeter.

A parameter which has been used for the form of the floes is the quotient of the greatest width and length. This is re: directly from the (1: 1 mill.) scenes.

Some of the imageries have been investigated in an additi. colour viewer in search for differences between one-year-ice and multiyear ice. This investigation was negative.

## RESULTS

### Form and dimensions of ice floes

Table 1 gives frequency distributions of the area of the ice floes encountered in various regions at various time of the year. Only floes with area greater than 10 $km^2$ have been considered. The Table indicates that for the ice passing through the Fram Strait from the Polar Sea there is a general trend of smaller floes becoming less frequent towards the summer. It is considered that this trend reflects the ongoing persistent disintegration, it is also seen that the number of floes greater than 100 $km^2$ decreases considerably in number from April to July. Note also the far greater number of such giant floes for 1975 than in 1976.

Seventeen of the nineteen graphs in Table 1 also indicate a bimodal distribution, showing a minimum in the areal coverage for floes of sizes between 40 and 80 $km^2$. The reason for a bimodal distribution is not known. Effect of swells is not a satisfactory explanation as this should apply to floes with an area less than 10 $km^2$.

From the Landsat imageries it was soon found that the ice broke up in a certain pattern, when there was a northerly airflow causing a southward transport of ice between the islands.

A typical example is shown in Fig. 1 which represents conditions with a north north-easterly wind. The figure reveals a lead pattern which is predominant in the area. Leads are seen to run from the maximum pressure zone along the islands towards the core of the ice flow. The direction of these leads is assumed to be perpendicular to the resultant force of the friction along the bounderies of the flow, and the wind stress. Should the patterns formed on each side of the core now and then overlap each other, floes may form with the parallelogram - like shape such as seen in great number in Fig. 1. The mentioned floe shape is also illustrated by Fig.2 where the direction of the ice flow is south-southwestwards along the continental slope north of Spitsbergen.

For the area represented by Fig. 1 the length and the width of a number of floes have been estimated. The relationship between these two lengths is shown in Fig. 3. The average quotient is seen to be close to 0.5. Fig. 2 shows also that this quotient is somewhat smaller in that area. It is assumed that this quotient depends upon the width of the strait as well as the strength of the forces involved.

Drift velocities and directions, and divergence.

From the material received it has been possible to obtain information on the ice drift conditions in a remote area of difficult access. Some of the floes have been recognized on the imageries over periods up to 15 days before they moved out of the investigated area. The movements of the ice floes within various periods have been noted on maps which are reproduced in the figures below.

Fig. 4 shows the drift observations obtained in 1975. Over a period of two days it is seen that the drift velocities in middle of April are around 25-30 cm $s^{-1}$, and that there is a convergence of ice in the Fram Strait. Considering a longer period, a divergence has been observed in this area (VINJE (1970)). It is therefore believed that the observed convergence is a temporary phenomenon.

Fig. 5 shows the displacement of ice floes during the period 21st April to 7th May 1976 together with borders of drift ice as well as land fast ice.

During the first part of the period there was a prevailing northerly wind in the area. The last part, however, was calm with fair weather caused by a high pressure area extending eastward from Greenland. The drift speed therefore generally decreases towards the end of the period. In the north-west of the Svalbard archipelago, the effect of the Vest-Spitsbergen current is evident.

The numerous icedrift estimations in the East Greenland Sea make it possible for the first time to determine the drift speed simultaneously at various locations across the Fram Strait From Fig. 6 it is seen that a maximum speed of about 25cm $S^{-1}$ is observed between $2^{o}E$ and $4^{o}W$ in the area between 80 and $81^{o}N$ The average speed through the strait is 20.5cm $S^{-1}$ during the period. As the width of the drift ice stream is 330 km, and the average thickness of the ice is around 3m thick, the outflow of ice from the Polar Ocean during the period 21.-27.April equals 0.2 Sv (1 Sverdrup = $10^{6}m^{3}$ $S^{-1}$). During the following period, 27.April - 2.May, the observations, though fewer in number, indicate that the outflow had decreased considerably to about 0,ISv, with an average speed of the outflow of about 10cm $S^{-1}$. The wind stress is relatively low in the area as well as over the Polar Ocean during the latter period, and the observed drift speeds may therefore indicate the velocity of the surface current.

A NIMBUS - 6 located automatic station was placed on an ice flow at $81^{o}N$ and $0^{o}W$ the 19.April. During the period 21.-27.April this station drifted approximately along the meridian at an average speed of 23,5cm $S^{-1}$. This is very close to the Landsat drift observations of about 25cm $S^{-1}$ (Fig.6.). Thus these two independent methods confirm each other.

The present material indicates that there may be great variations in the drift speed from floe to floe within a given area. On one occasion a certain floe became relatively isolated from the other floes with compareable dimensions. This floe, indicated by IF in Fig.5, is seen to move very different from the others in that area. The average speed for this particular floe during the period 21.-27.April, is 31cm $S^{-1}$ or 40% higher than the speed of the other floes which is 22cm $S^{-1}$. The reason for this may in the part be that the ice floe had an exceptional shape both above and below the water surface.

When the drift ice in the Trans Polar Current passes into the East Greenland Sea considerable acceleration takes place. For the period 27.April to 2.May the observation in the centra area (80-81°N, 0-4°W) noted in Fig.6, shows that the average speed increased from 11.1cm $s^{-1}$ at 80.8°N to 21.4cm $s^{-1}$ at 80.1°N. The divergence in this area was $2.7 \times 10^{-7}$ $s^{-1}$ for the five-days period. This corresponds to an opening up of as much as 10-12% of a given area over this short period. At this time of the year open water at these latitudes may re-freeze. Because of this effect as well as the acceleration in speed, it becomes very important to select the proper measuring line when the outflow from the Polar Sea is to be estimated.



The acceleration observed during the calm period 21.-27. April in the core of the flow is not indicated in the observations from adjacent areas during the period 27.April to 2.May when there was prevailing notherly winds.This may either indicate that the location of maximum acceleration is very fixed, which seems unreasonable, or that it may be dependent upon the wind stress. The latter assumption is in the present case supported by observations as Fig.7 shows that when the export of ice is increased by the wind stress the area of maximum acceleration is found north of the center of the passage.

Fig. 7 shows drift speed observed in the eastern part of the archipelago on the 24.-25.April. The highest speed, 54cm $s^{-1}$, is found for a floe moving along the local ice edge (cf. fig.1). A considerable acceleration and divergence take place also here where the ice flow passes through the strait between Kvitøya and Storøya. The width of the strait between the two islands is 58km. With an average speed of 25cm $s^{-1}$, a thickness of 3m and a concentration of about 70% the out-flow becomes 0.03 Sv. This amounts to 15% of the out-flow through the Fram Strait as estimated above for the period 21.-27.April. The width of the passage between Kvitøya and Semlja Franza Iosifa is about 120 km. For similar condition in this area we can estimate a total out-flow of ice from the Polar Sea between Greenland and Semlja Franza Iosifa of about 0.29 Sv. for the period considered. The estimated figures must be considered as an upper value as the out-flow was favoured by north-north-easterly winds.

Fig. 8 show the observed displacements of floes in the northern part of the Greenland Sea for May 1976. The weather conditions for this month were very variable in the area. There was, however, a predominance of easterly and southerly winds up to 19. May, from then to 22. May there was north-westerly winds and then variable light winds for the rest of the month.

It may be assumed that easterly and southerly winds have a neutral or retarding influence on the southward directed flow in the East Greenland Current. It is therefore of particular interest to study conditions with such an atmospheric circulation. The observed drift velocities for the period 5.May - 16.May are reproduced in Fig.9 together with the observed direction of drift. There are some local maxima which at least partly may be due to the rapid movements of special floes as observed above.In the major maximum zone the speed of the drift is 13.7 cm $s^{-1}$ on an average, decreasing towards west to 7-10cm $s^{-1}$. It is noted that the observed maximum zone coincides more or less with the continental slope in the area,cf.Fig.10.Note also the anticyclonic circulation to the west and the cyclonic one to the north-east.

The May observations show a convergence of $17 \times 10^{-7}$ $s^{-1}$ at 80.5°N - 9°W, 20.-24.May, $0,4 \times 10^{-7}$ $s^{-1}$ at 79,5°N - 2°W, 10-14. May, $4.6 \times 10^{-7}$ $s^{-1}$ at 78.2°N - 5°W, 5.-9.May and $0.5 \times 10^{-7}$ at 78,5°N - 12° W,12.-16.May. This indicates that an increase in concentration and ridging should have taken place in the area during the periods. This is probably caused by the effect of the wind conditions described above.

Fig. 11 represents the drift observations obtained in the area north and east of Svalbard. North of the islands there is a general trend of west north westward movements, at speeds between 4 and 7cm $s^{-1}$. The direction is in accordance with east south easterly winds prevailing during the first part of May.

A convergence of $4 \times 10^{-7}$ $s^{-1}$ is found for the flow. It is of interest to note the change in direction of drift through the passage between Nordaustlandet and Kvitøya in the middle of May. This occurs in close accordance with the change in the wind direction during the same period. The wind speed is estimated to be relatively weak and the observation therefore indicates that the drift of ice through this passage is mainly governed by the wind stress (for the considered period).

According to climatic studies of the area (STEFFENSEN (1969) the amount of fog and clouds generally increases markedly through June and July. This was also the case for 1976 and relatively few Landsat imageries have been obtained for this period.

Fig.12 shows the drift observations obtained in the Fram Strait during June and July. A striking feature is the anti-cyclonic circulation of the ice floes which seems to have developed markedly since May. A high pressure condition pre-vails over the area with very weak winds. There is found to be a divergence between 3 and $6 \times 10^{-7} s^{-1}$ at $80.2^{o}N-2^{o}W$ and at $80^{o}N-12^{o}W$.



The unexpected anticyclonic circulation should be compared with the special ice conditions. This year there was an extraordinary big area of open water at the north-east coast of Greenland at the end of July and the largest eastward extension of sea ice between $75^{o}$ and $77^{o}N$ in the Greenland Sea, for the last 11 years (VINJE (1977)). This indicates that special oceanographic conditions prevailed during the considered period.

Fig. 13 shows the drift observations in the eastern part of the Svalbard archipelago. The permanent currents in this area are very complex according to PREOBRAZHENSKIY (cf. NOVIT-SKIY (1961)). His current chart, which is based on dynamical calculations, is reproduced in Fig. 14. The period 5.-8. July starts with calm weather on 5. and 6. July and the correspond-ing drift speed of 10cm $s^{-1}$ south of Kong Karls Land may be considered as the surface speed of the current. On the 7th and 8th there is a south westerly air current with a speed of 5-15 kts. The retarding effect of this wind is clearly seen from the observations in the coastal East Spitsbergen current (cf. Fig.14.). There is one observation from the 9th in this area which shows a change in drift direction. This corresponds with an approach of a low with winds from south west of about 15-25 kts. At these winds velocities the direction of the ice drift may be determined by the wind. Fig. 15 reproduces two Landsat scenes (2503-10543 and 2503-10545) to show the complex current system which may be visualized in brash ice over the shallow shelf in the south eastern part of the archi-pelago.

## The operational ice charts at the Norwegian meteorological service compared with Landsat imageries

The operational ice charts of the Norwegian meteorological service are mainly based on NOAA strips (SR). Ground truth data are very scarce from the area in question.

It soon became evident that for conditions of high cloud cover the weather satellites are inferior to Landsat for determination of the ice conditions. On 26.August 1975, for instance, the Landsat imagery 2216-14303 indicated an ice concentration of 3/8 through a thin cloud-veil. On the weather satellite-based ice charts the concentration was for the same time estimated to be as high as 6-7/8.

A more detailed discription will be given below for three cases in 1976.

The 5th of May the surface weather maps showed SE wind in the area (cf. Fig.17.). This wind direction had prevailed for several days, with a force between 10 and 30 kts. In such a case with "on-shore" winds the ice edge will be well defined and easy to locate on the pictures. We note the relatively broad area with brash ice as well as the indication of the surface water in an area with neighbouring currents of opposite direction.

The Landsat imageries for 6.May (Fig.16.) as well as the NOAA SR strip both reveal a well defined ice edge west of Spitsbergen. The map with plots of the two edges shows, however, rather large differences,up to 90km. This must be due to inaccurate position on the NOAA-based ice charts.

The 10th of May the wind was still "on-shore" in the area but had turned to ENE. Both types of satellite images show a distinct ice edge west of Spitsbergen (Fig.17.). The plots of the edges show good agreement, except for the many more details in the Landsat imageries. In this case, the difference in position of the two edges does not exceed 30-40 km.

The weather maps for 21.-22.May show conditions entirely different from the previous two. A low pressure north of Spitsbergen directs a west or west north westerly air current over the area, with a speed of 20 kts. on 20.May decreasing to 5 kts. on 22. May, cf. Fig. 18.

The distinct edge has disappeared, and it is difficult to determine the position of the edge from the Landsat imageries, somewhat easier on the NOAA strip. The wind is "off-shore" and we note the remarkable difference in the ice boundary zone. The zone is 50-100 km wide and reveals a pattern in the brash ice which must be caused by wind and ocean currents (cf. Fig. 18 with fig. 16.).

The different cases shown are typical for the differences between Landsat and NOAA ice analysis. The differences are mainly due to difficulties in exact tracing of the ice edge from the NOAA SR strips on to the ice charts.

The comparison above is somewhat out of date, as VHRR (and next year A VHRR) will be the main source of information for mapping the sea ice. There may, however, still be problems of exactly tracing the ice edge from the imageries.

## The influence of the wind on the ice conditions near the edge

The aim was to estimate from Landsat scenes the movement of the ice edge over 2-3 consecutive days and compare this movement with wind data. No attempt has been made to take ocean currents into consideration, because little is known of their speed and direction in the investigation area. All cases shown are from the eastern and southern part of the Svalbard archipelago.

The weather maps give the isobaric situation and some plotted observed winds in the area. In general, the arctic stations on Eastern Greenland and in Svalbard are non-representative with respect to winds for most directions. In particular this is the case for Longyearbyen and for Jan Mayen Instead of the observed winds the geostrophic winds measured on the weather maps is therefore used. The true winds deviate from the geostrophic wind by some 25 degr to the left. On the other hand the drift of the ice will be to the right of the wind (some 15 degr according to theory). Taking also into account the uncertainty of the isobars in these areas it seems reasonable to use the geostrophic wind in connection with the study of sea ice movements.

The maps, pictures and figures given below for each case will be self evident, and just a few comments are necessary.

The conditions during the period 23.-25.April 1976 are represented in Fig. 19. The wind speed is about 25 kts. and the direction is north east backing slightly north north-east during the period. The edge of the sea ice is moved from north east at an average speed of 15 km per day. This corresponds to a drift velocity of about 1.4% of the geostrophic wind speed.

The conditions during the period 12.-13.May 1976 are represented in Fig. 20. In this case the wind is rather weak, 6-8 kts and north north east. The ice edge drifts towards the south at an average speed of 5 km per day. This corresponds to 1.5% of the speed of the geostrophic wind.

The conditions for the period 26.-28.May 1976 are represented in Fig. 21. Landsat scenes for 27. May are missing, so we consider here the movements over two days. The weather maps show that the wind has been westerly ,20 kts, the first day, later north westerly 25-30 kts, decreasing to 12-15 kts. An average wind is estimated to west north west 20 kts. The displacement of the sea ice is approximately 25 km in two days, which gives an ice drift which corresponds to 1.4% of the estimated geostrophic wind speed.

The conditions for the period 29.-30.May 1976 are represented in Fig. 22. The mean wind is north west, later north east, 10 kts. The displacements are 5-10 in the western part. This gives an average drift velocity of 1.2 - 2,2% of the estimated geostrophic wind speed.

The conditions for the period 16.-19. May 1976 are represented in Fig. 23. This case is somewhat different as it starts with south westerly winds, which causes a relatively small stress towards north on the ice edge. The ice edge moves, however, southwards and this is in all probability an effect of the sea currents which may be observed when the wind speed is relatively low (cf Fig. 13 and 14and the discussion).

During the period 17.-19.May the wind speed increases to 25 kts from south east, veering to south. The mean geostrophic wind for these two days are estimated to be southerly 25 kts. The displacement of the ice edge ranges from 25 km in the eastern part to 10 km in the western part. This drift corresponds to about 1-2,2% of the geostrophic wind speed.

The Landsat scene for 19. May shows (in the southwestern part) how the ice react on different wind directions. For several days there has been "off shore" winds, bringing the ice some 20-30 km towards south. With the southerly wind the ice is moved northwards again, and it is clearly seen that a new edge is formed. (Fig. 23 contd.)

The above investigation shows that the ice edge in the eastern part of the Svalbard archipelago on an average is displaced with a speed which amounts to about 1,5% of the geostróphic wind speed normal to the edge. This is a little less than given by textbooks, namely 2%, and may be due to a retarding influence on the drift of the islands in the area. It can be mentioned that the percentage, 1,5%, found above is conformed by several other comparisons made from the material available.



A comparison with ground truth data

With regard to Fig. 1 surface observations were made a couple of hours before the imagery was obtained. A flight at a low height was performed along the northern coast line of Nordaustlandet and across the sea between Storøya and Kvitøya where a NIMBUS - 6 automatic station was deployed on land fast ice. The observed concentration of sea ice in the over-flown area is very much like the concentration indicated by Fig. 1. The darker areas in the drift ice as well as on the snowcovered islands are in all probability caused by shadow effects from thin cirrus stratus which were observed that particular day.

The fast ice west of Kvitøya where the airplane landed, was soaked with salt water. A closer study on an additive colourviewer turned out no significant differences between this snow and snow on thick winter or multi-year ice. It is therefore not believed that salt content may help in determining the age of the drift ice.

## SIGNIFICANT RESULTS

As the present investigation area is remotely situated and not easily accessible, particularly during the cold season, it becomes clear that Landsat imageries will give original information of great interest. The present investigation indicates unexpected great variation in the drift velocity of the ice in the Fram Strait. During calm weather the southward directed speed is observed to be 10cm $s^{-1}$ at $81^{O}N$ at the end of April 1976. About a week later during conditions with northerly moderate winds the speed increased to about 20cm $s^{-1}$. For this period it was also possible, for the first time, to determine the drift velocity at various positions across the Fram Strait. The speed in the core, between $2^{O}E$ and $4^{O}W$, was observed to be about 25cm $s^{-1}$. The corresponding export of ice from the Polar Sea, which through the Fram Strait amounts to 70-90% of the total is estimated to be $0,2\times10^{6}m^{3}$ $s^{-1}$ A marked acceleration as well as a divergence is observed when the ice passes southward through the straits both west and east of Svalbard. The present investigation therefore gives important information of value also for future measuring schemes for monitoring the outflow of sea ice from the Polar Sea.

A predominance of parallelogram-like floes was observed during the early spring, and for the whole period April-July there seems to be a minimum areal coverage of floes of an average size of about 60 $km^2$.

A remarkable anticyclonic circulation is observed in the Fram Strait in May ,June and July. It is noted that this coincides with extreme distribution of the drift ice in that area when comparing with the last ten-years period.

The speed of the displacement of the ice edge in the eastern part of the archipelago corresponds to about 1.5% of the geostrophic wind velocity.

It soon became evident that the NOAA strips (SR) are inferior to Landsat imageries for determination of sea ice conditions. Very great discrepancies may occur particularly during periods with high cloudiness. On 26 August 1975, for example, an ice concentration of 3/8 was determined from Landsat while 6-7/8 was estimated from the SR.

Compared with surface observations from air planes it is found that sea ice concentrations in the area are in accordance with Landsat-based determinations. It is further found from investigation on an additive colour viewer that salt soaked fast ice does not show any significant contrast compared with ordinary snow covered sea ice or land ice of various ages.

## CONCLUSIONS

The Landsat imageries have demonstrated their unique utility within a number of diciplines. This becomes of special importance for institutes which are in charge of investigations in not easily accessible polar areas.
In the daily work with sea ice the Landsat imageries constitute a source for unique information, which also in the future will become an important source of reference in connection with increasing economic exploration in the area.

## ACKNOWLEDGEMENTS

This report has been prepared in co-operation with Mr O. Bremnes at the Norwegian meteorological institute.
Mr Ø. Finnekåsa at the Norwegian Polar Research Institute has prepared the photoproducts and extracted the necessary back ground material for the investigation.

## REFERENCES

NOVITSKIY, V.P., 1967: Postoyannyye techeniya severnoy chasti Barentseva Morya (Permanent currents of the Northern Barents Sea). Trudy Gosudarstvennogo Okeanograficheskogo Instituta Vol. 64, pp. 1-32. Leningrad

NYE, J.F., and D.R. THOMAS, 1974: The use of satellite photographs to give the movement and deformation of sea ice. AIDJEX BULLETIN No. 27. Seattle.

STEFFENSEN, E., 1969: The Climate and its Recent Variations at the Norwegian Arctic Stations. Met. An. Vol. 5. No. 8, Oslo.

VINJE, T.E., 1970: Some observations of the ice drift in the East Greenland Current. Norsk Polarinstitutt Årbok 1968. Oslo.

-"- , " 1977: Sea ice conditions in the European sector of the marginal seas of the Arctic 1966-1975. Norsk Polarinstitutt. - Årbok 1975. Oslo.

Table 1
Frequency distribution of the area of ice floes at various sites and at different time of the year.



1975
EAST GREENLAND CURRENT

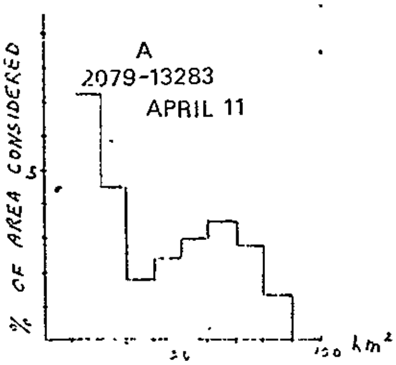


AREA CONSIDERED: 14545 km²
164 FLOES ≥ 10 km²
21 FLOES ≥ 100 km²
GREATEST FLOE: 1070 km²
OPEN SEA: 15%

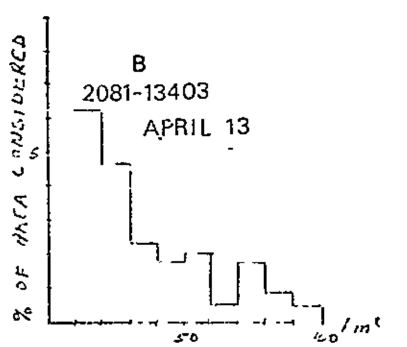


AREA CONSIDERED: 26882 km²
259 FLOES ≥ 10 km²
29 FLOES ≥ 100 km²
GREATEST FLOE: 986 km²
OPEN SEA: 15%

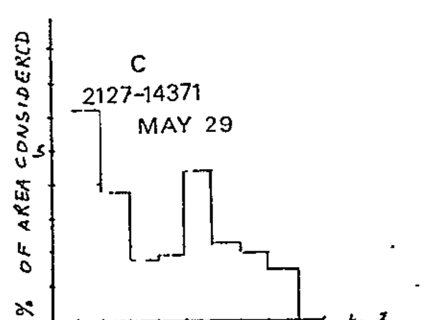


AREA CONSIDERED: 23977 km²
205 FLOES ≥ 10 km²
16 FLOES ≥ 100 km²
GREATEST FLOE. 587 km²
OPEN SEA. 20%

1976
EAST GREENLAND CURRENT

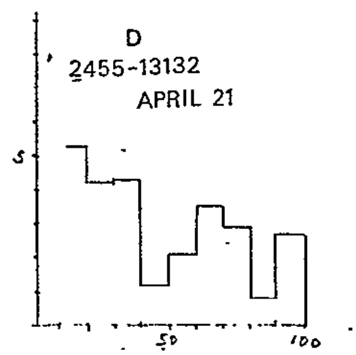


AREA CONSIDERED 10545 km²
110 FLOES ≥ 10 km²
16 FLOES ≥ 100 km²
GREATEST FLOE: 1160 km²
OPEN SEA: 15%

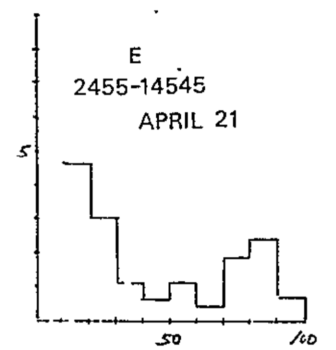


AREA CONSIDERED: 14084 km²
89 FLOES ≥ 10 km²
4 FLOES ≥ 100 km²
GREATEST FLOE: 225 km²
OPEN SEA: 15%

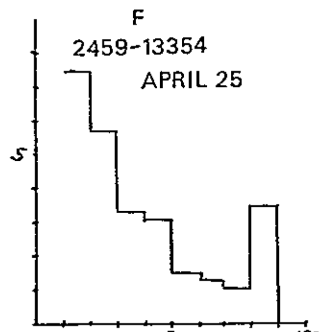


AREA CONSIDERED: 14952 km²
174 FLOES ≥ 10 km²
15 FLOES ≥ 100 km²
GREATEST FLOE: 325 km²
OPEN SEA: 20%

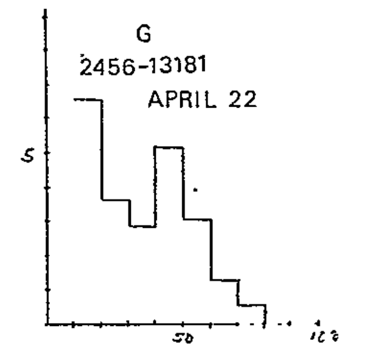


AREA CONSIDERED. 14211 km²
123 FLOES ≥ 10 km²
3 FLOES ≥ 100 km²
GREATEST FLOE: 263 km²
OPEN SEA. 15%

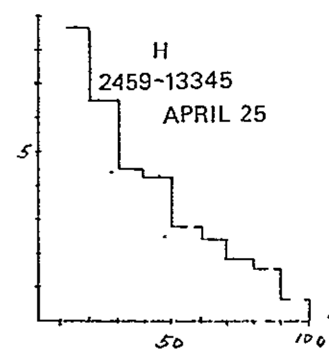


AREA CONSIDERED. 15860 km
198 FLOES ≥ 10 km²
3 FLOES ≥ 100 km²
GREATEST FLOE: 200 km²
OPEN SEA. 15%

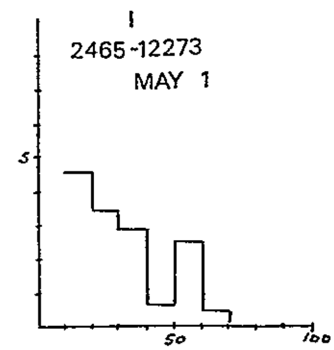


AREA CONSIDERED: 12961 km²
86 FLOES ≥ 10 km²
4 FLOES ≥ 100 km²
GREATEST FLOE: 371 km²
OPEN SEA: 20%

Table 1,continued.



1976
EAST GREENLAND CURRENT

1976
EAST OF SVALBARD

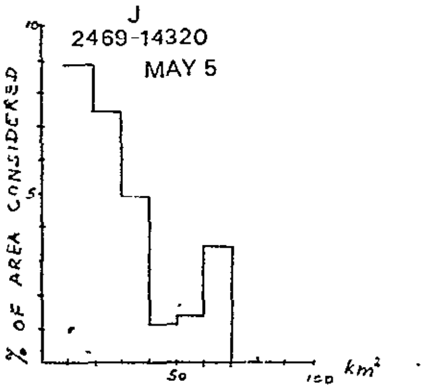


AREA CONSIDERED: 7575 km²
95 FLOES ≥ 10 km²
3 FLOES ≥ 100 km²
GREATEST FLOE: 383 km²
OPEN SEA: 10 %

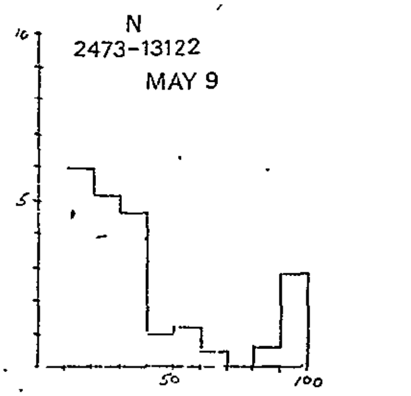


AREA CONSIDERED: 13192 km²
123 FLOES ≥ 10 km²
5 FLOES ≥ 100 km²
GREATEST FLOE: 544 km²
OPEN SEA: 20%

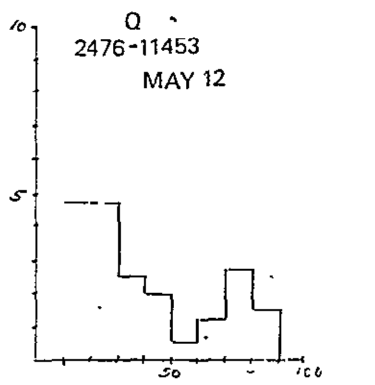


AREA CONSIDERED: 11[illegible] km²
85 FLOES ≥ 10 km²
1 FLOE ≥ 100 km²
GREATEST FLOE: 119 km²
OPEN SEA: 15%

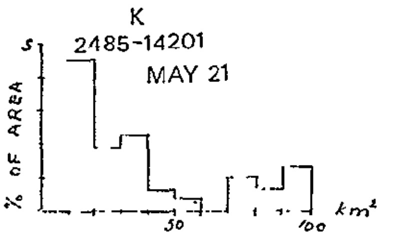


AREA CONSIDERED: 13925 km²
81 FLOES ≥ 10 km²
6 FLOES ≥ 100 km²
GREATEST FLOE: 275 km²
OPEN SEA: 20%

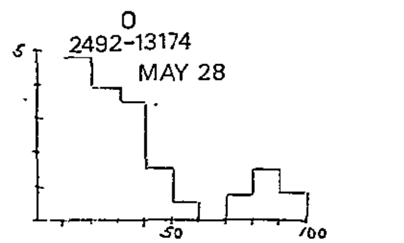


AREA CONSIDERED: 11325 km²
83 FLOES ≥ 10 km²
7 FLOES ≥ 100 km²
GREATEST FLOE: 988 km²
OPEN SEA: 20%

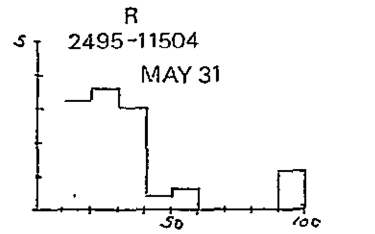


AREA CONSIDERED 9173 km²
52 FLOES ≥ 10 km²
2 FLOES ≥ 100 km²
GREATEST FLOE: 441 km²
OPEN SEA: 10%

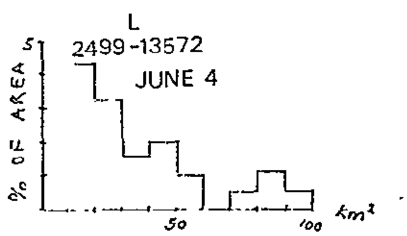


AREA CONSIDERED: 15350 km²
93 FLOES ≥ 10 km²
5 FLOES ≥ 100 km²
GREATEST FLOE: 213 km²
OPEN SEA: 20%

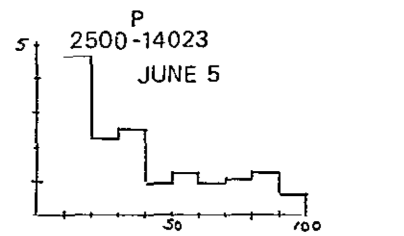


AREA CONSIDERED: 14755
96 FLOES ≥ 10 km²
7 FLOES ≥ 100 km²
GREATEST FLOE: 1400 km²
OPEN SEA: 30%

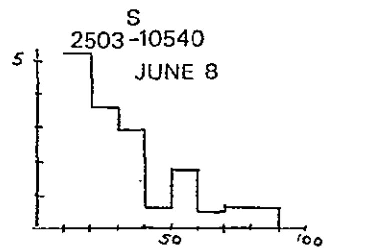


AREA CONSIDERED: 12960 km²
94 FLOES ≥ 10 km²
6 FLOES ≥ 100 km²
GREATEST FLOE: 318 km²
OPEN SEA: 15%

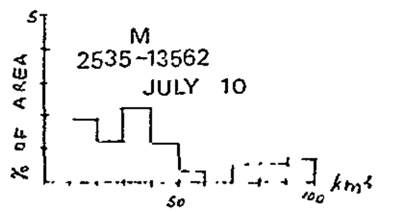


AREA CONSIDERED: 16220 km²
56 FLOES ≥ 10 km²
4 FLOES ≥ 100 km²
GREATEST FLOE: 270 km²
OPEN SEA: 30%

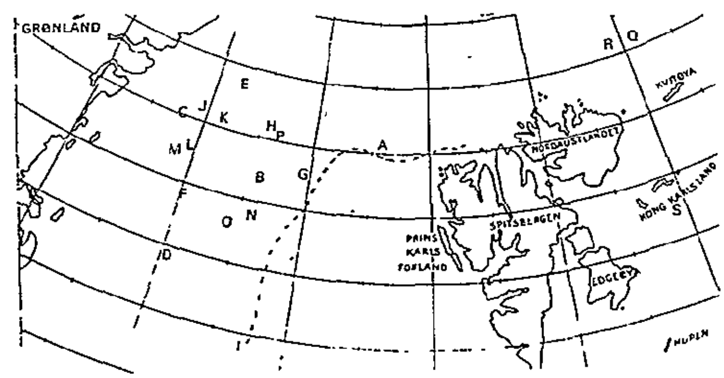

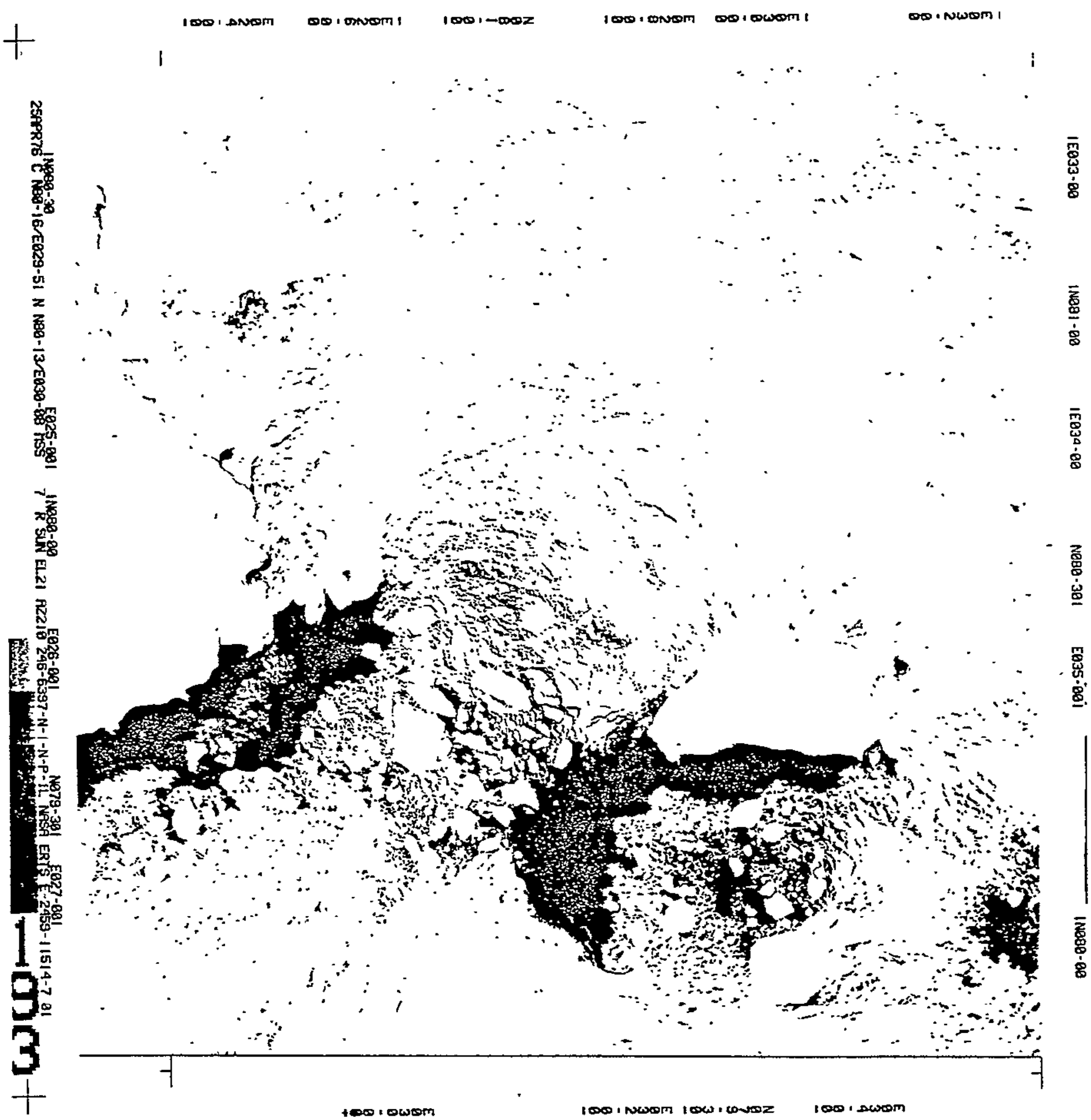


Fig. 1

Imagery obtained in the eastern part of the Svalbard archipelago 25 April 1976. There is a strong drift of ice from north northeast through the passage between [illegible]

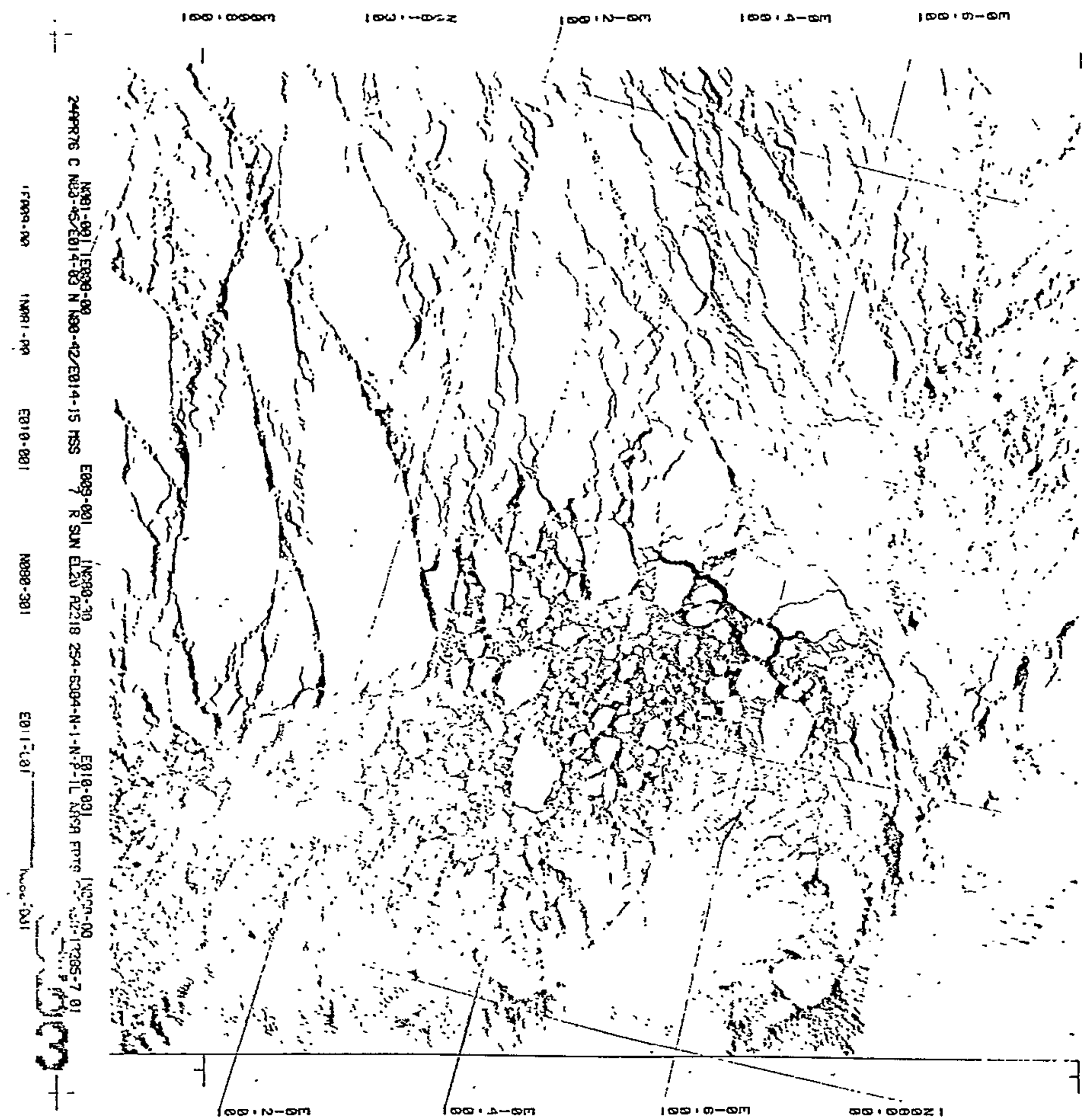

Fig.2
Floes with a paralellogram-like shape north-west of Spitsbergen 24 April 1976.

ORIGINAL PAGE IS
OF POOR QUALITY

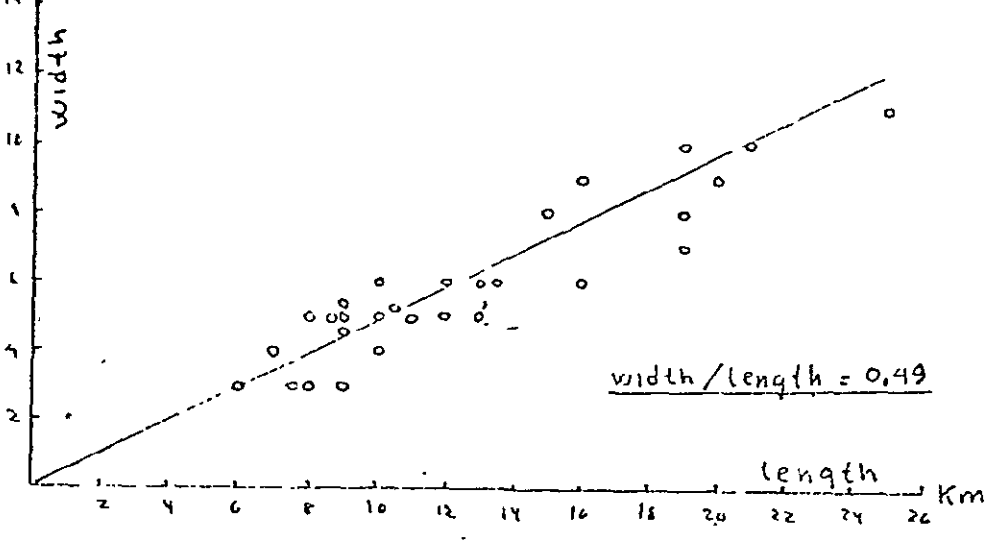


Fig. 3

Relationship between length and width of ice floes in an area of outflow represented in Fig. 1.

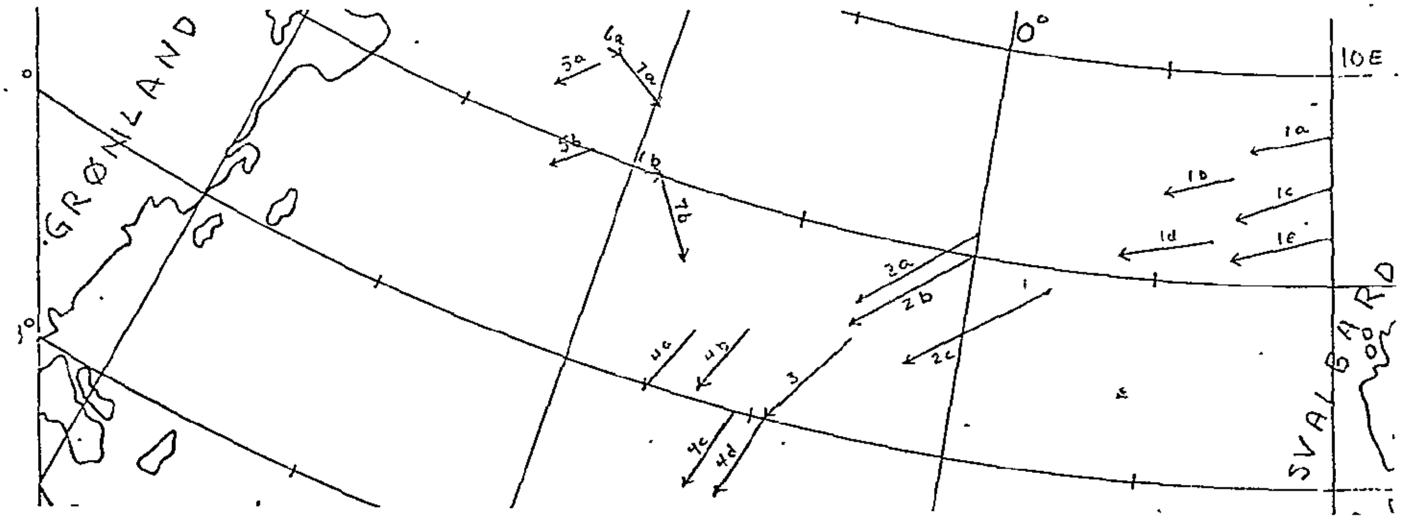


| Ref. | LANDSAT ID | Period | Velocity cm/sec | Divergence sec$^{-1}$ |
|---|---|---|---|---|
| 1 | 2077-13171..2079-13283 | 9 APR -11 APR-75 | 25 | $-1.0\cdot10^{-6}$ |
| 2 | 2077-13173..2081-13403 | 9 APR -13 APR | 25---31 | $-3.0\cdot10^{-6}$ |
| 3 | 2077-13173..2079-13292 | 9 APR -11 APR | 25---31 | $-3.0\cdot10^{-6}$ |
| 4 | 2077-13292..2081-13403 | 11 APR -13 APR | 25---31 | $-3.0\cdot10^{-6}$ |
| 5 | 2076-14544..2077-15002 | 8 APR - 9 APR | 27---35 | $-1.0\cdot10^{-5}$ |
| 6 | 2216-14303..2217-14361 | 26 AUG -27 AUG | 14---23 | |
| 7 | 2217-14361..2229-14021 | 27 AUG - 8 SEP-75 | 7---10 | $2.6\cdot10^{-5}$ |

Fig. 4

LANDSAT-based drift and divergence calculations.

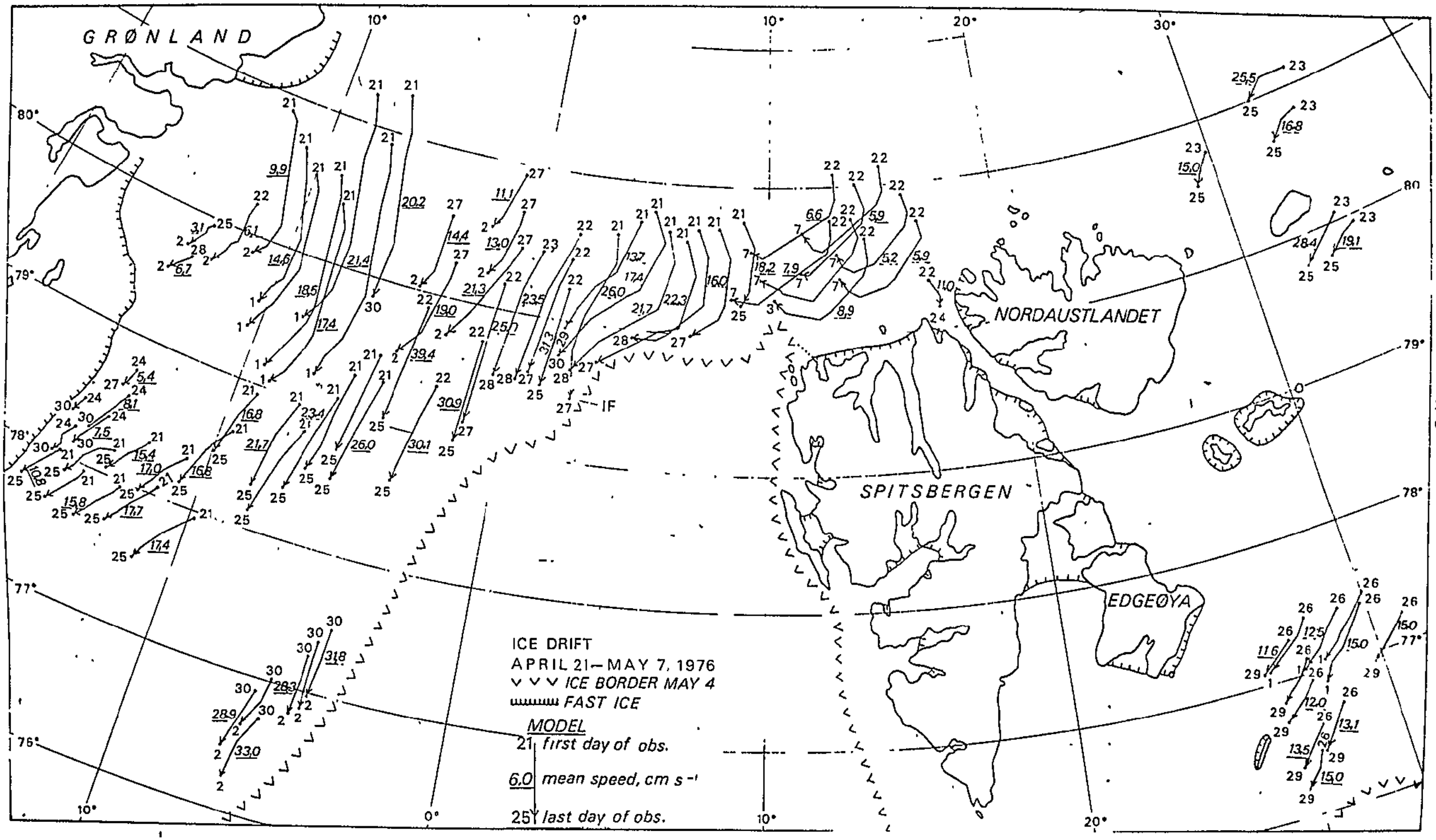


Fig.5

Ice drift observations for 21 April-2 May 1976. Note the irregular drift of the floe marked IF.

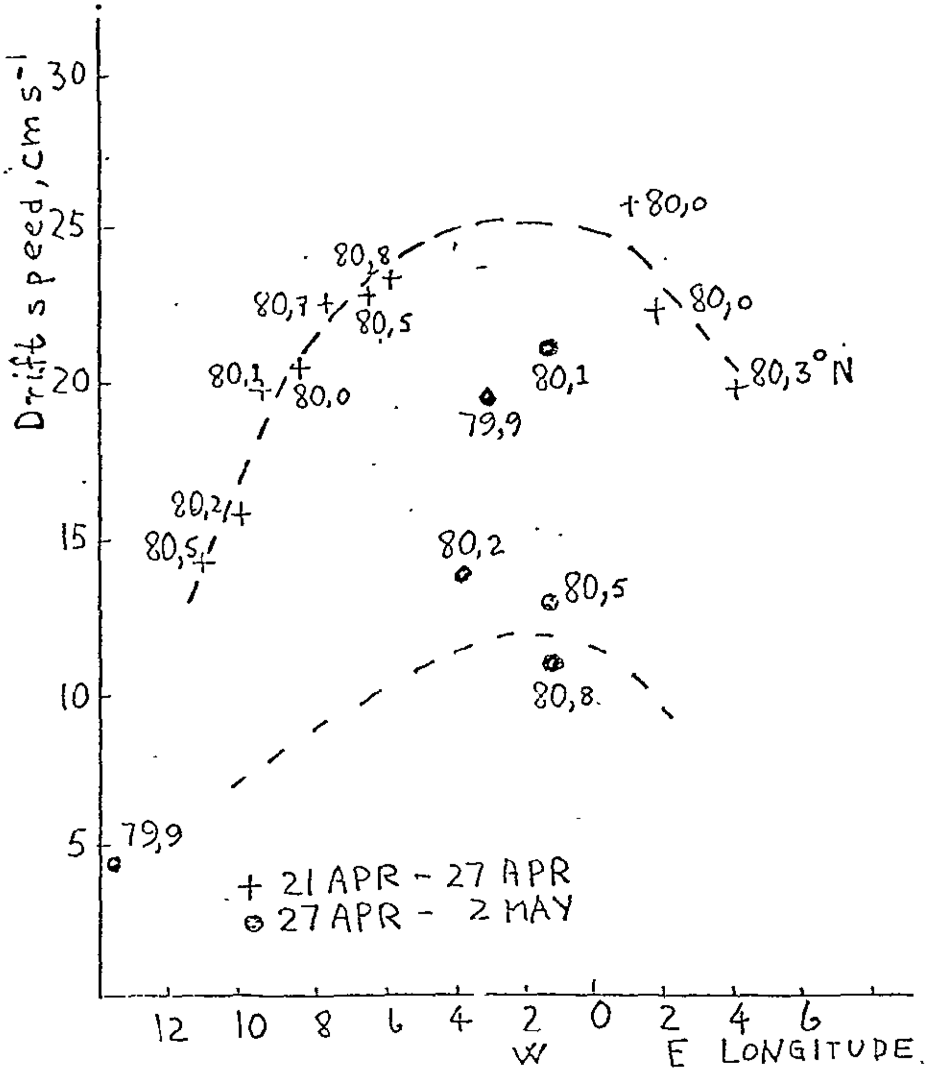


Fig.6

Drift speed of ice floes in the Fram Strait during the period 21 April-2 May 1976.The latitude is given for the average location of the floes considered.

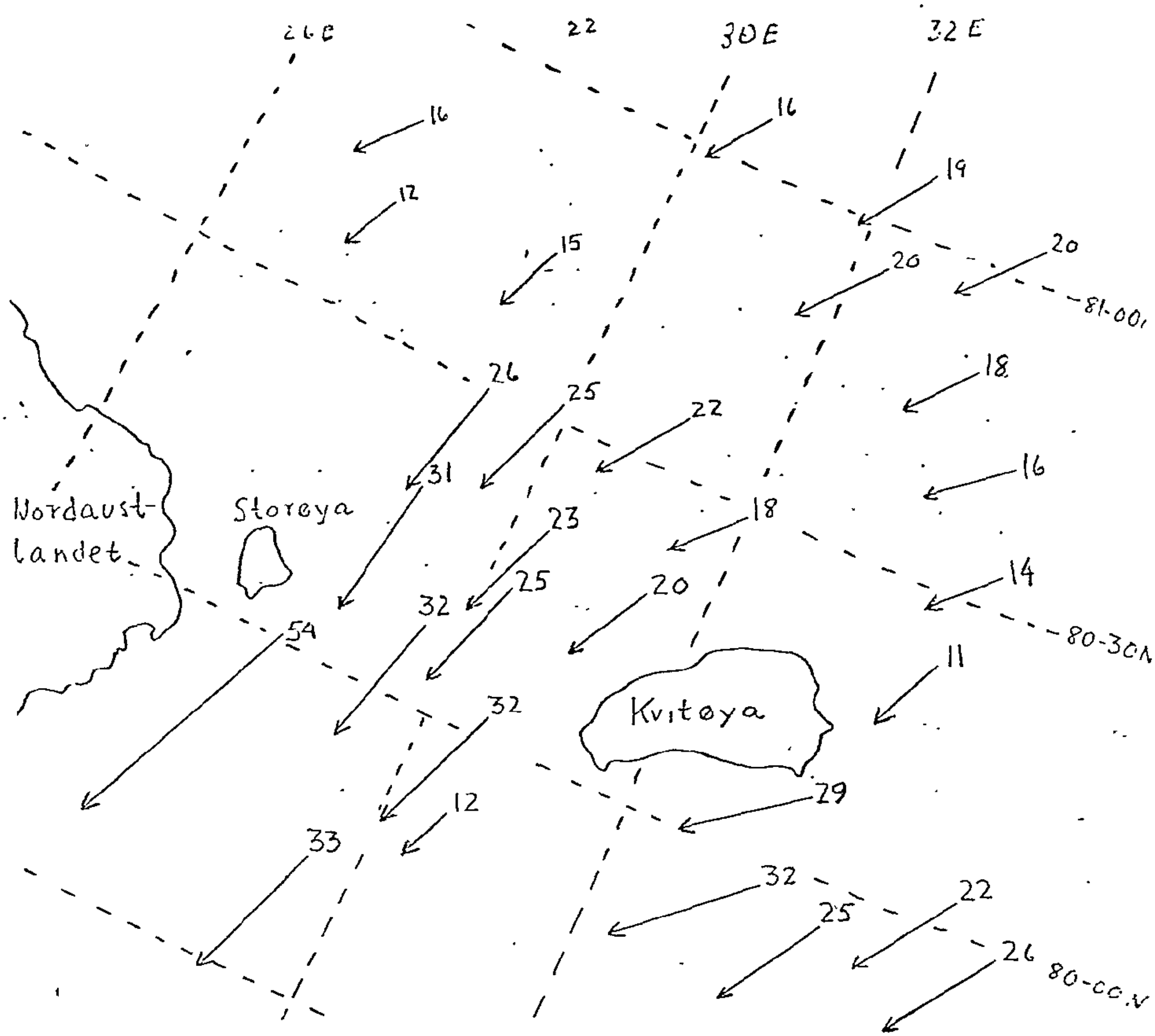


Fig.7
Drift speed ,cm $s^{-1}$, of floes from 24 to 25 April 1976
in the area represented by Fig.1.

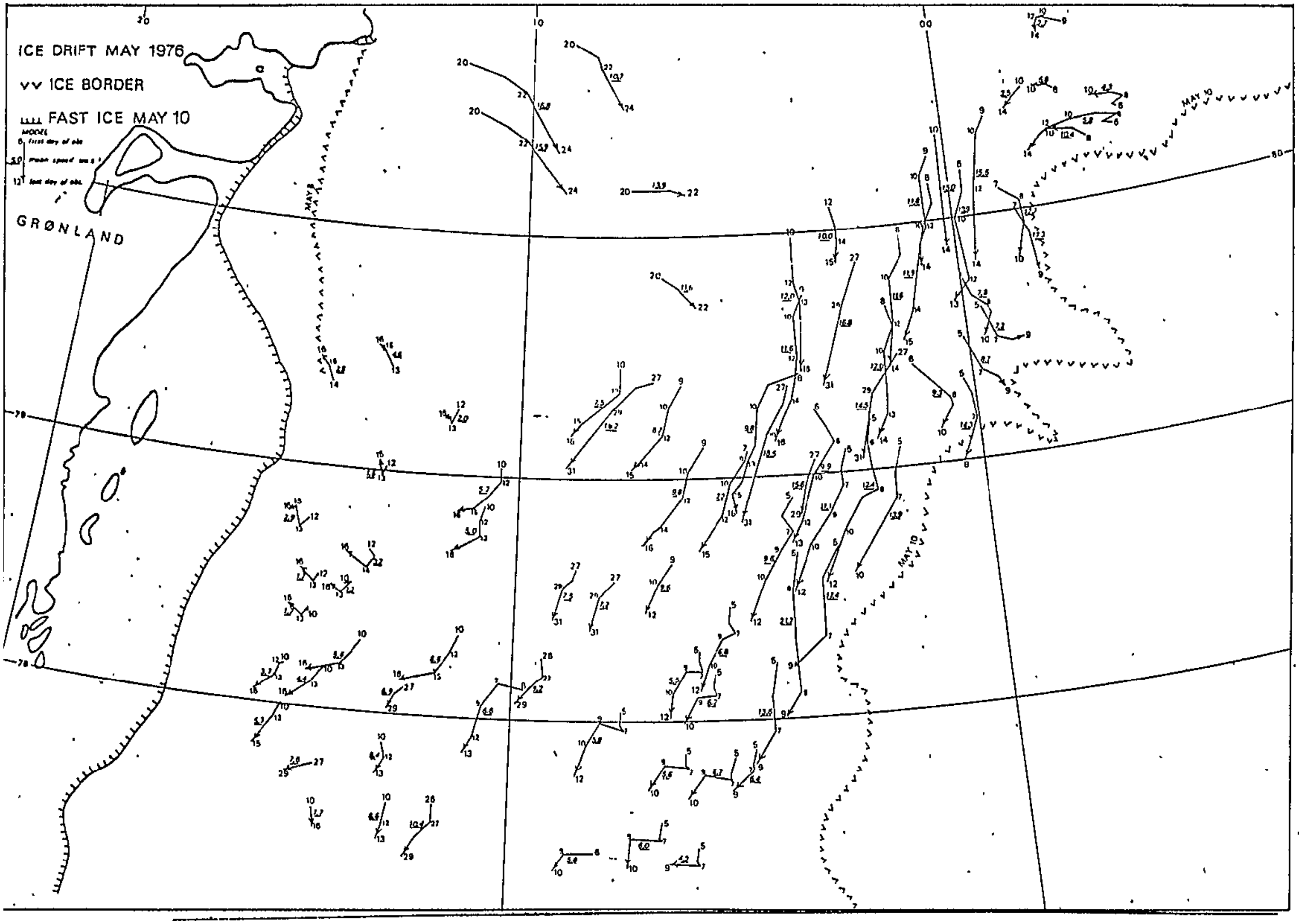


Fig.8
Ice drift observations for May 1976.

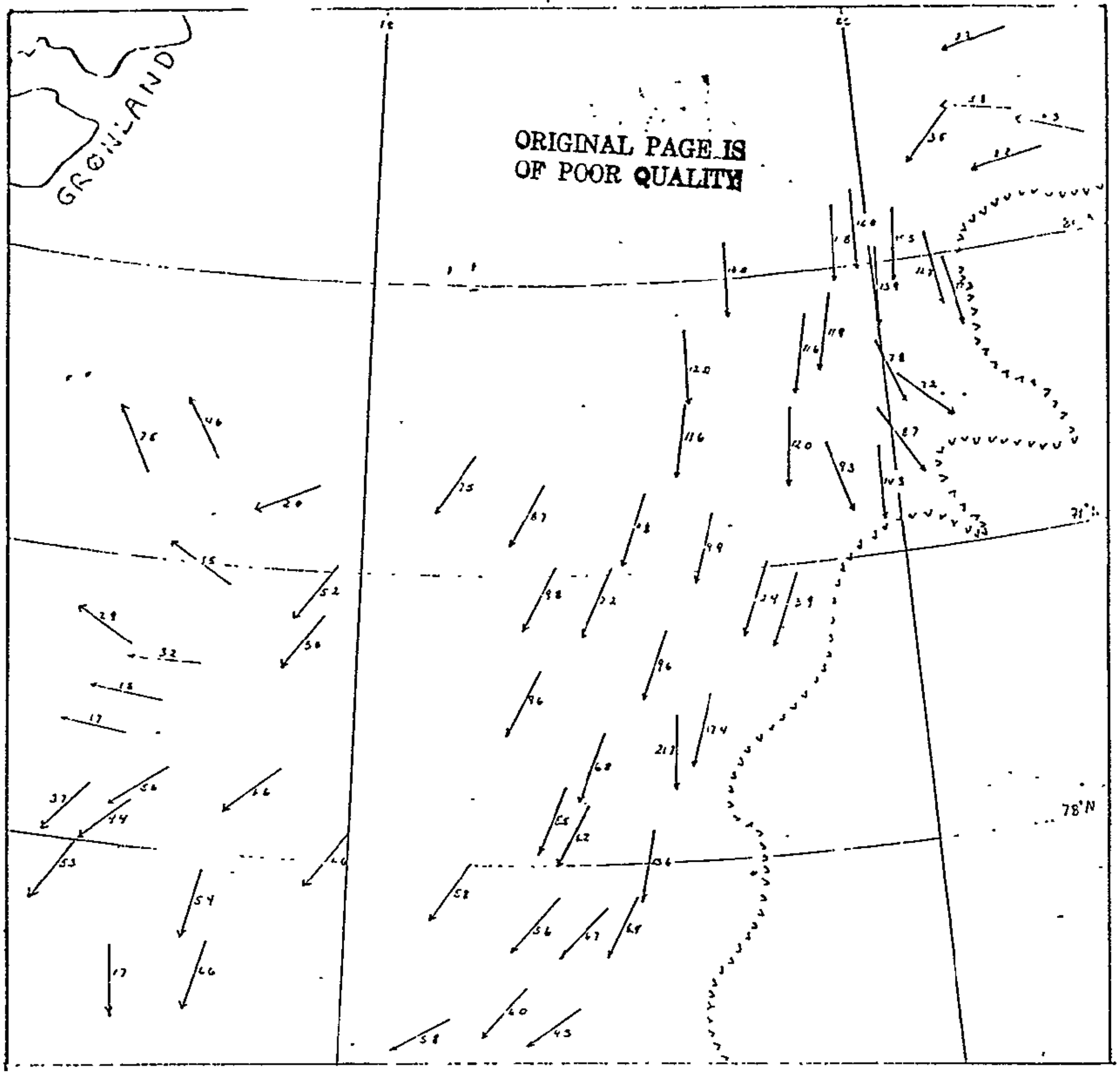




Fig. 9

Direction and drift speed of ice floes for the period 5 - 16 May 1976. Note the anticyclonic circulation to the west and the cyclonic circulation in the northwest.


Fig. 10

Bathymetric chart of the investigation area.

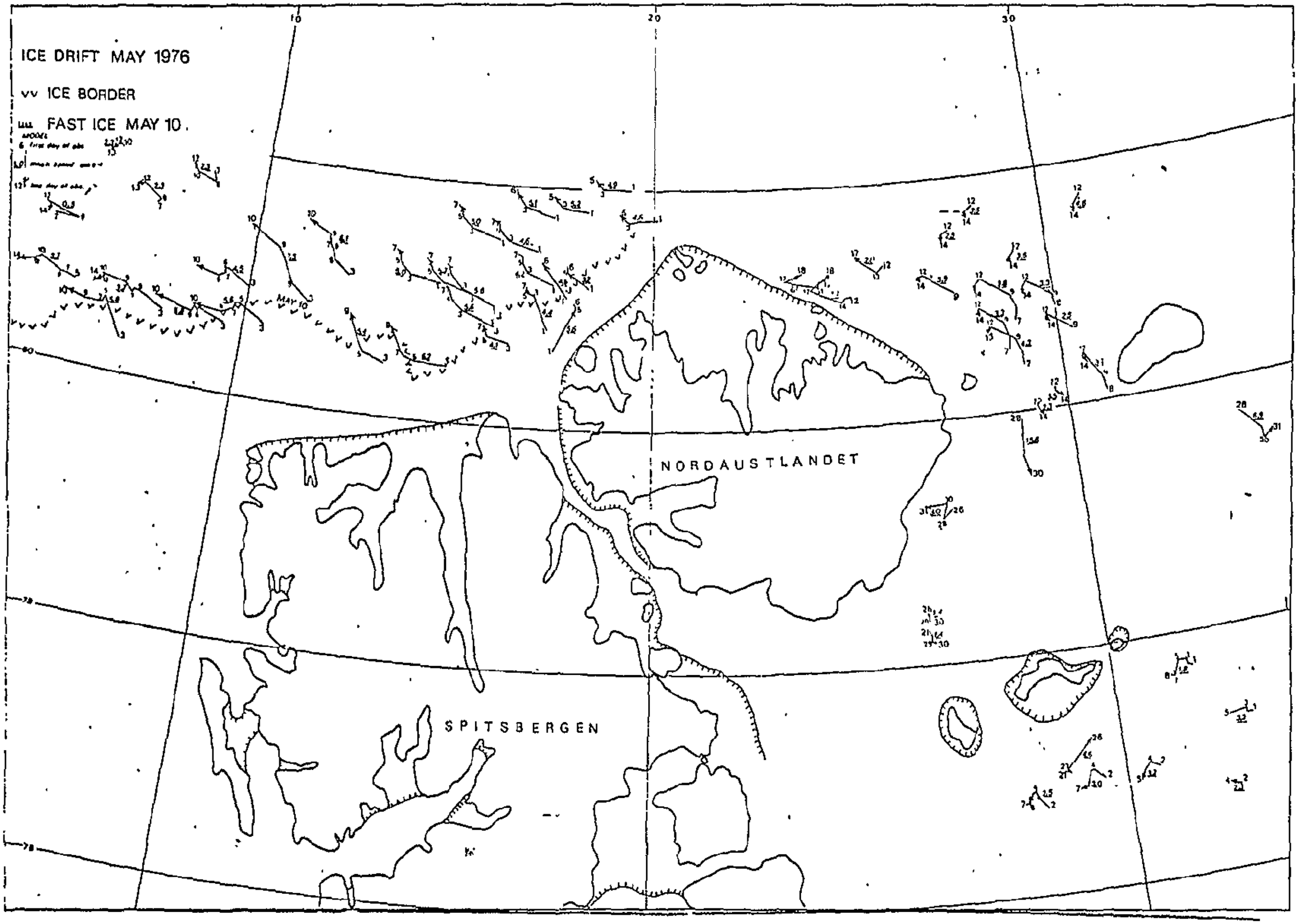


Fig.11
Ice drift observations for May 1976.

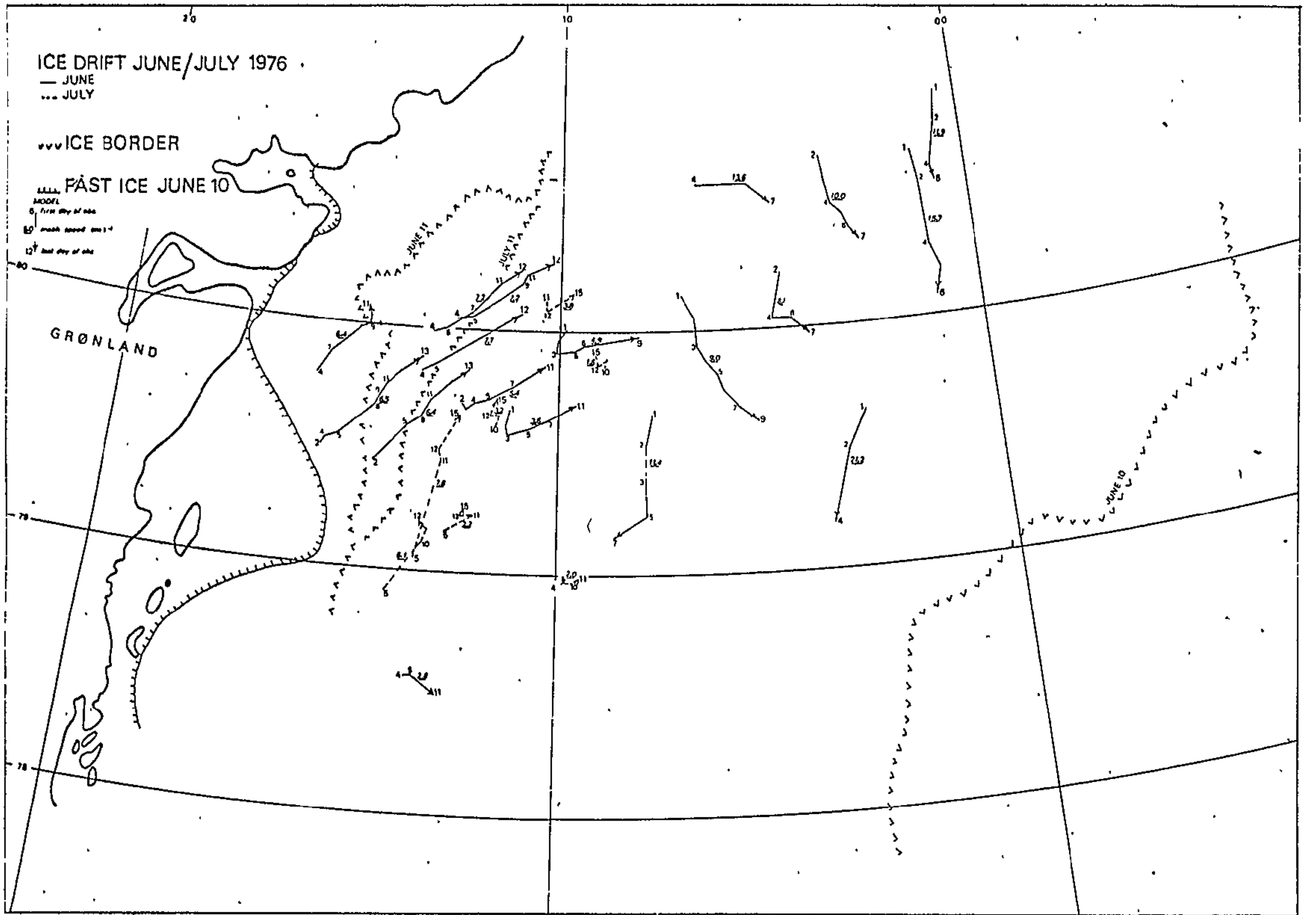


Fig. 12
Ice drift observations for June and July 1976.

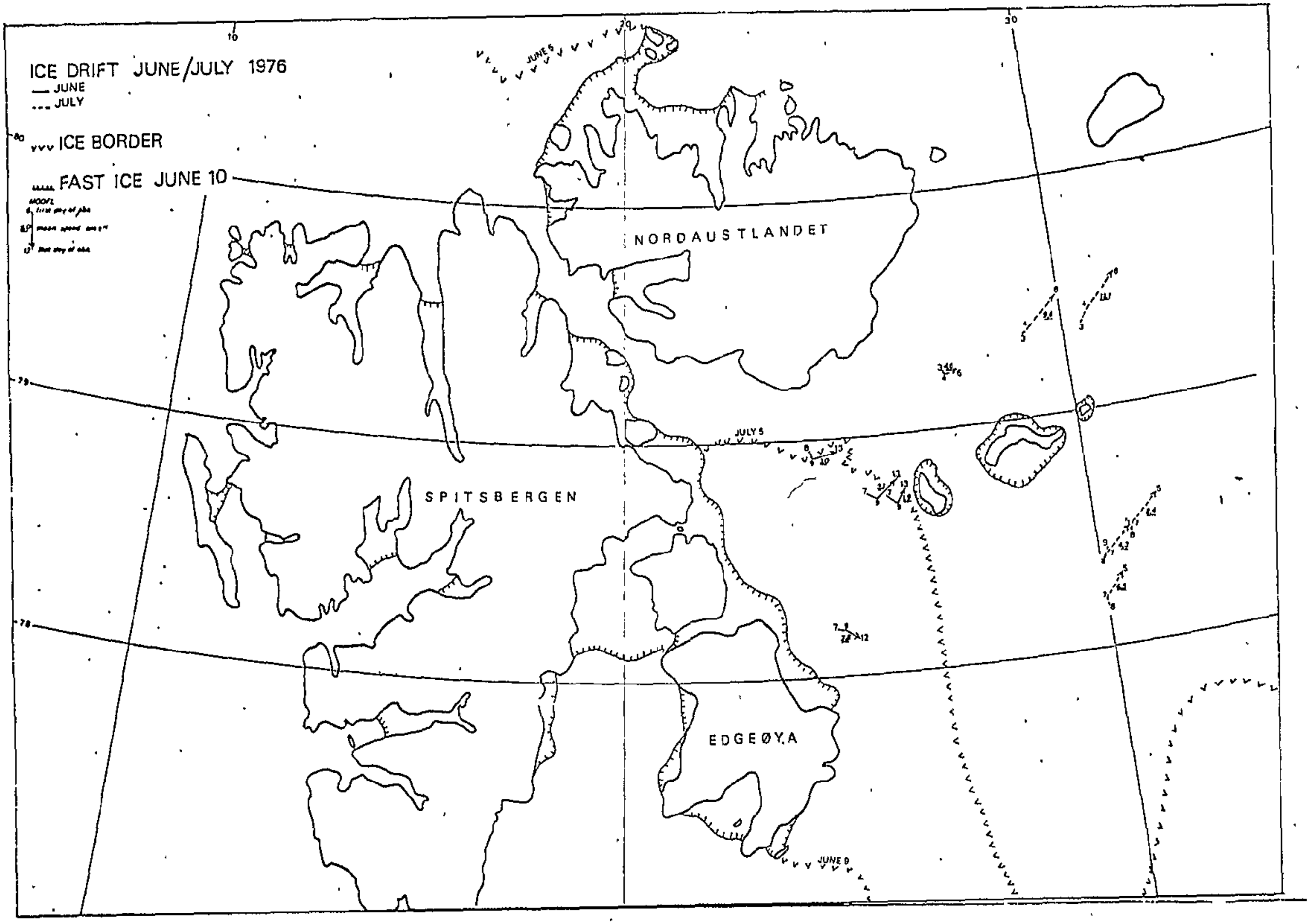


Fig.13
Ice drift observations for June and July 1976.

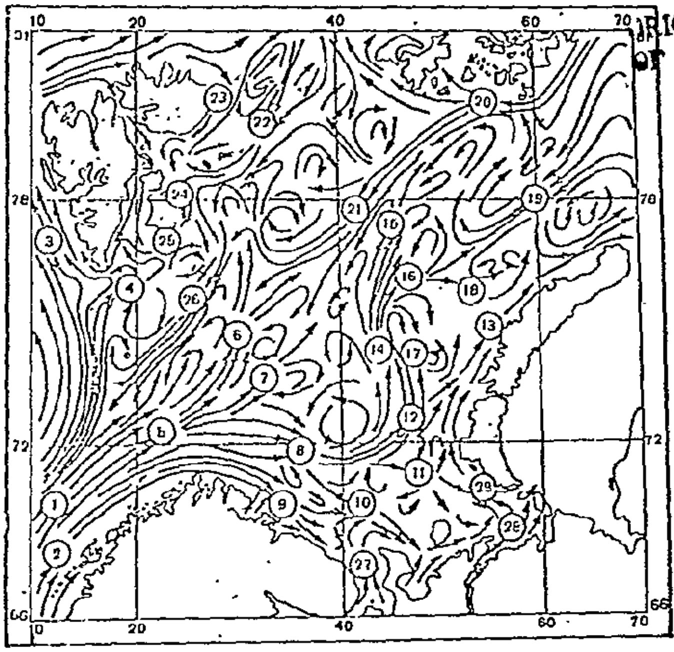

~~FIG. 11~~. General Scheme of Water Circulation of the Barents Sea, According to Yu. V. Preobrazhenskiy (southern part) and V. P. Novitskiy (northern part).

1 - E branch of Norwegian Current
2 - coastal Norwegian Current
3 - W Spitsbergen Current
4 - S Spitsbergen (Sørkapp) Current
5 - Nordkapp Current
6 - N Branch of Nordkapp Current
7 - Central (Middle) Branch of Nordkapp C.
8 - Murman Current
9 - coastal Murman Current
10 - Kanin Branch of the Murman Current
11 - Kolguev Branch of the Murman Current
12 - Novaya Zemlya Current
13 - coastal N. Z. Current
14 - NW Nov. Z. Current
15 - N Central Current
16 - N Nov. Z. Current
17 - Nov. Z. Banka Current
18 - Gorbovyye ostrov Current
19 - Arctic Trough Current
20 - Coastal C. of Franz Josef Land
21 - SW Current (Persey C.)
22 - E Spitsbergen Current
23 - Nordaustlandet Current
24 - Coastal E Spitsbergen C.
25 - Sørkapp Branch of E. Spitsbergen Current
26 - Hopen-Bjornøya Current
27 - White Sea Runoff Current
28 - Pechora Current
29 - Litke Current

Fig.14
Circulation in the Barents Sea according to dynamic calculations.

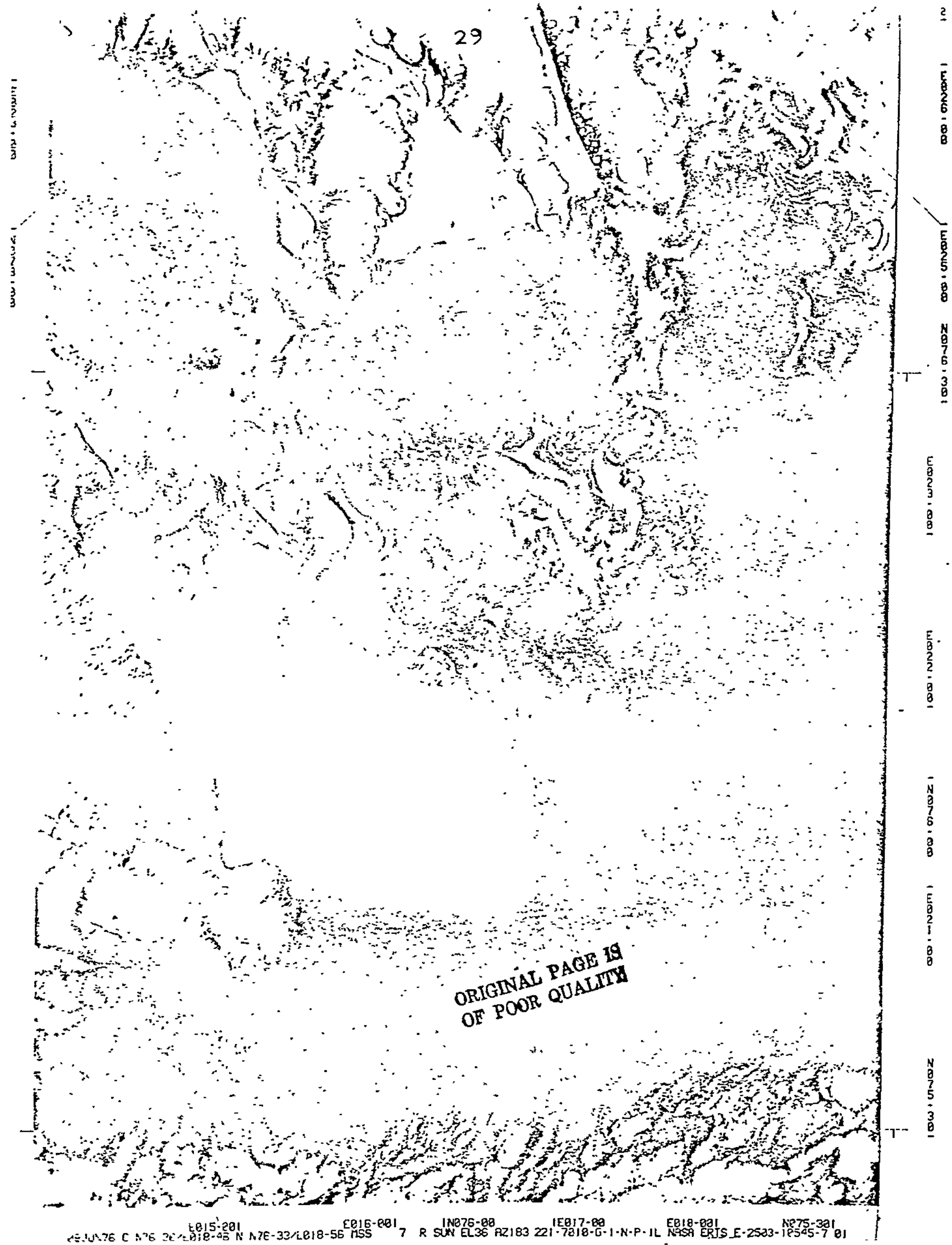




Fig.15

Complex current system as visualized in brash ice in the southern part of the Svalbard archipelago 8 June 1976.

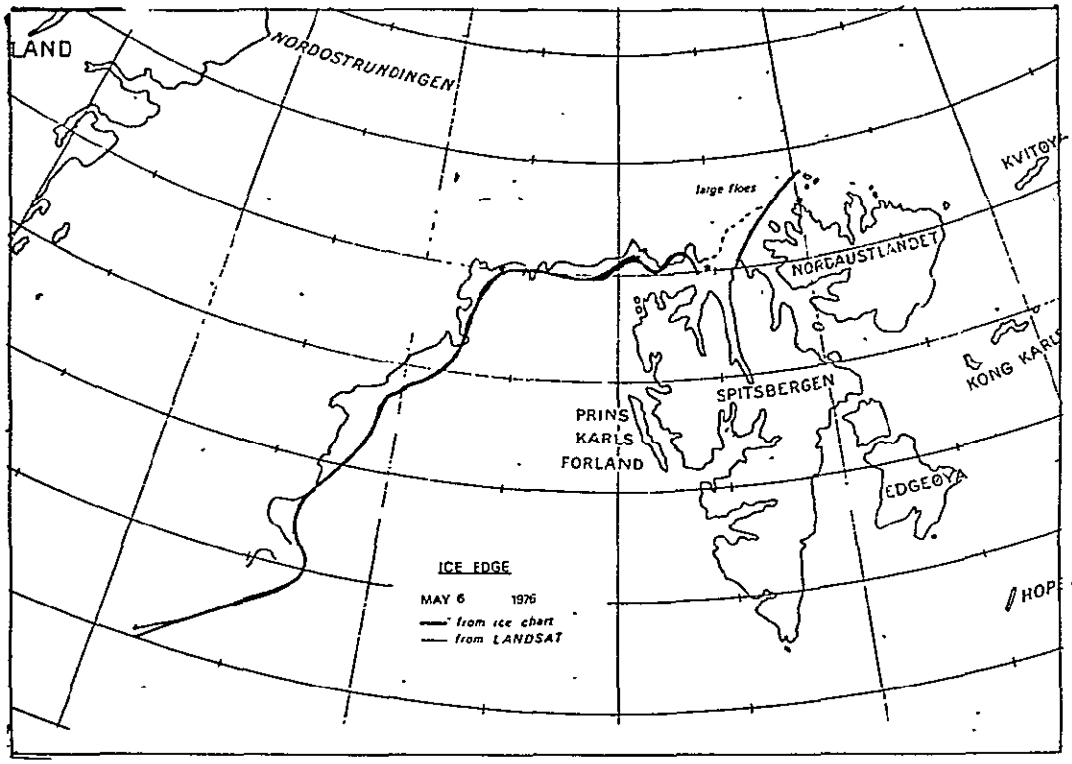


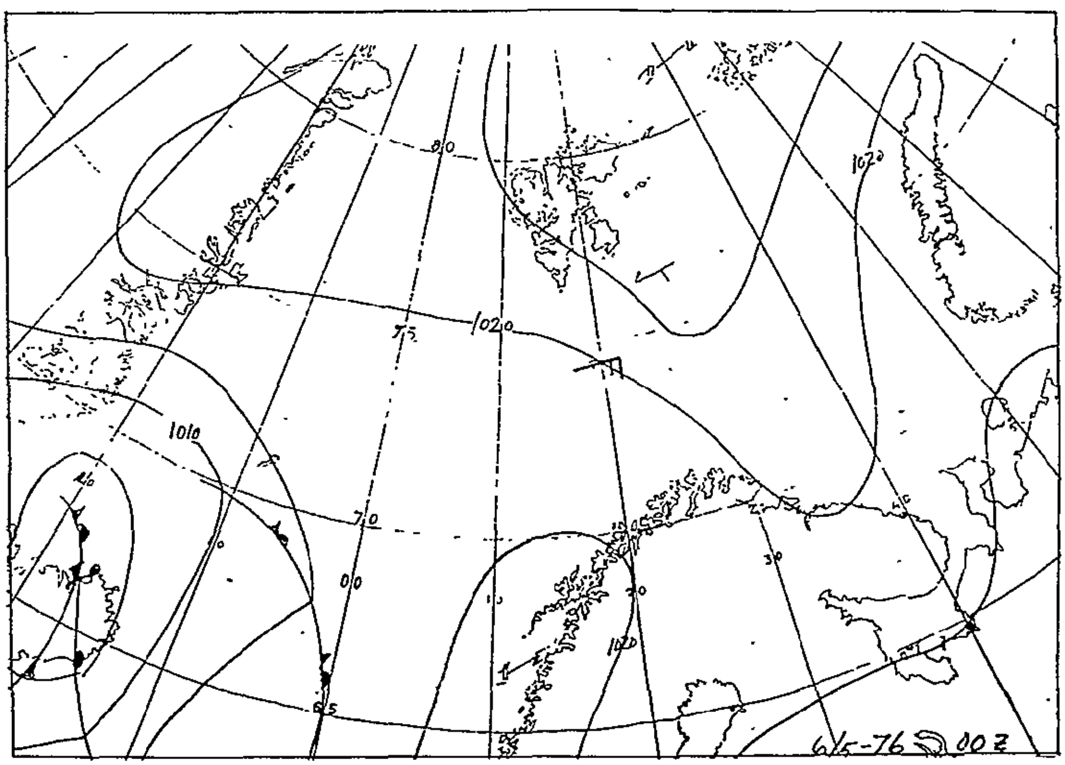


Fig.16

Landsat ice edge compared with ice chart and weather map 6 May 1976.

31

ORIGINAL PAGE IS OF POOR QUALITY

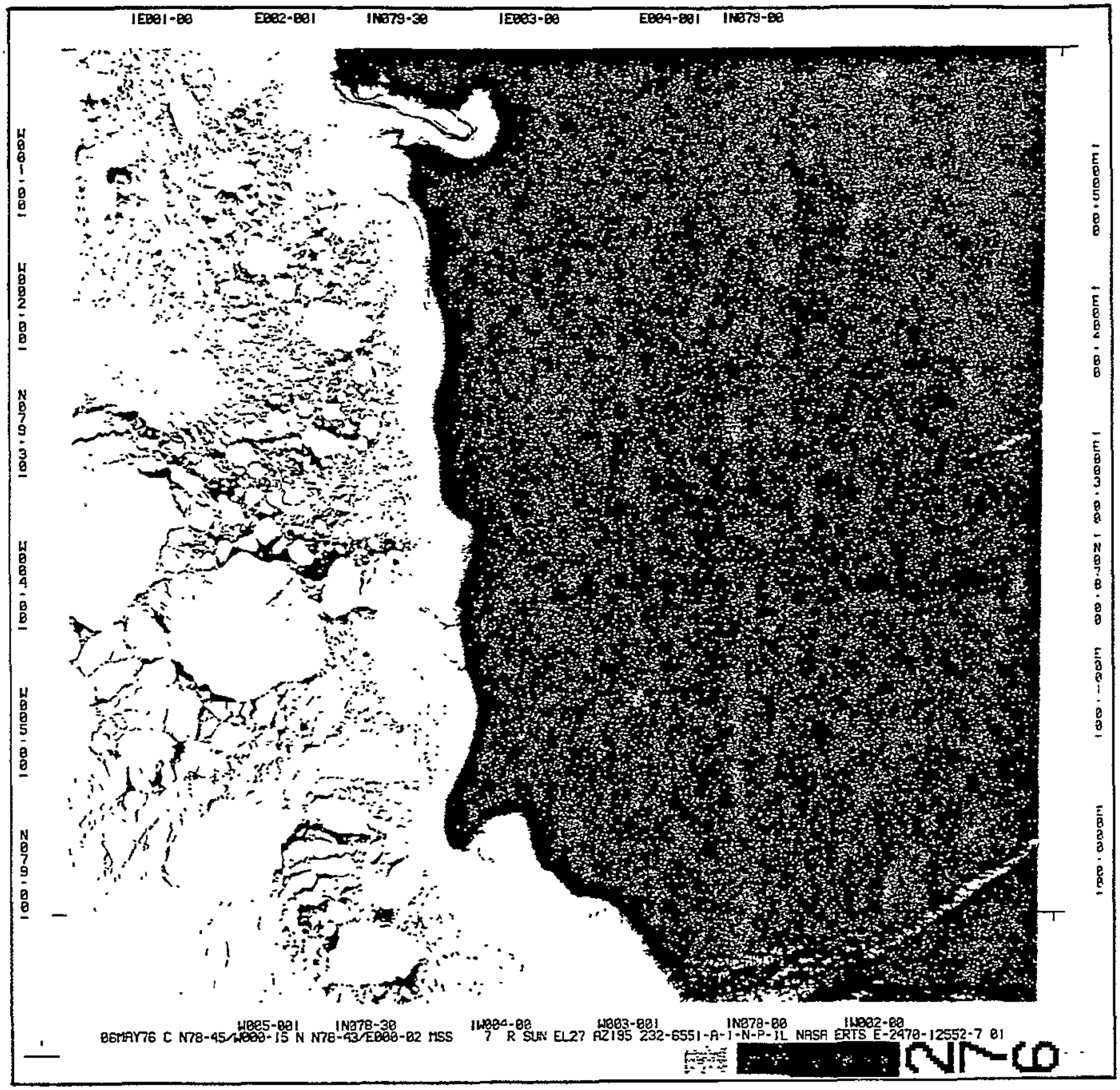

Fig.16 contd.
Characteristic ice edge during conditions with wind blowing towards the ice edge.

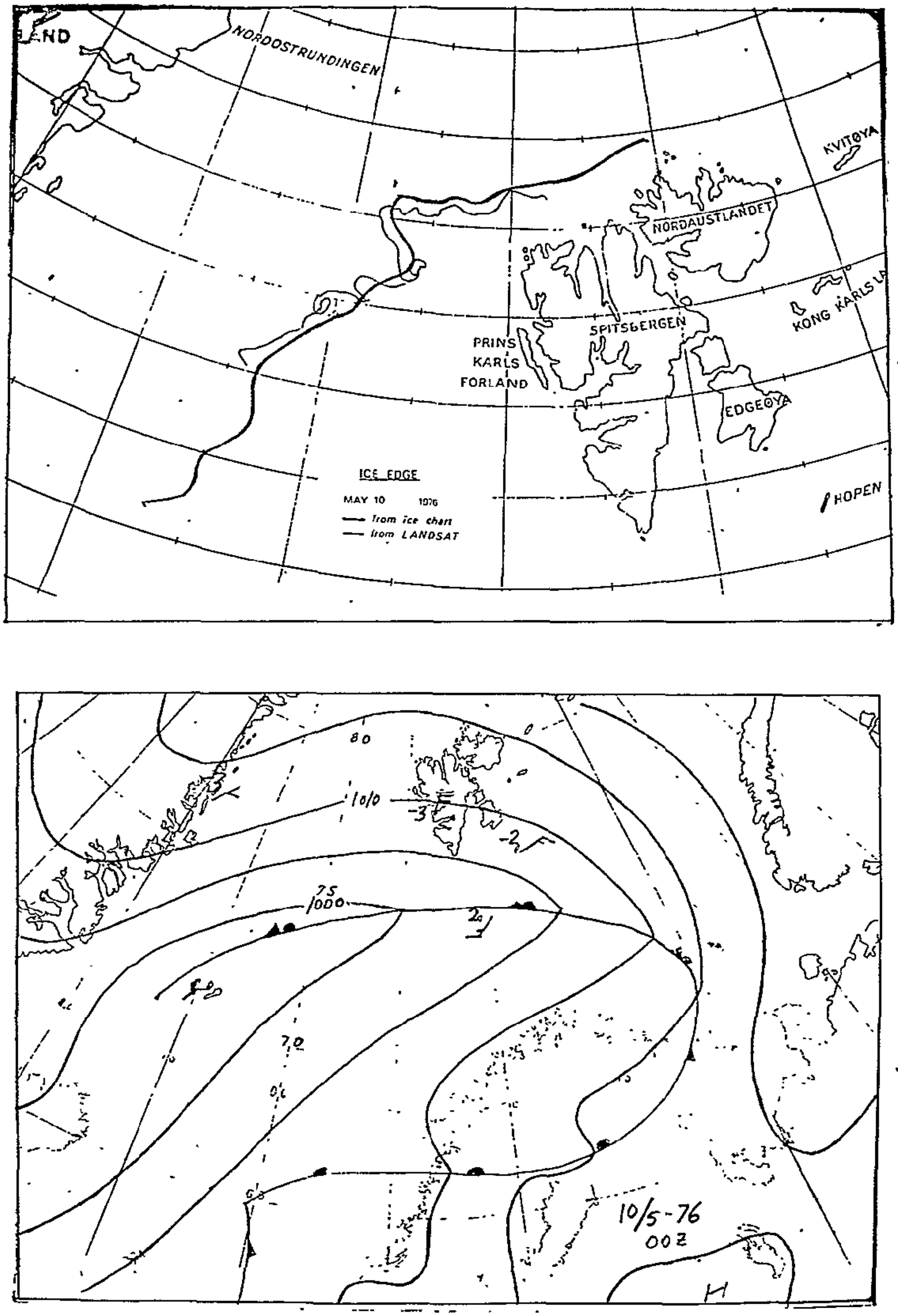


Fig.17

Landsat ice edge compared with ice chart and weather map 10 May 1976

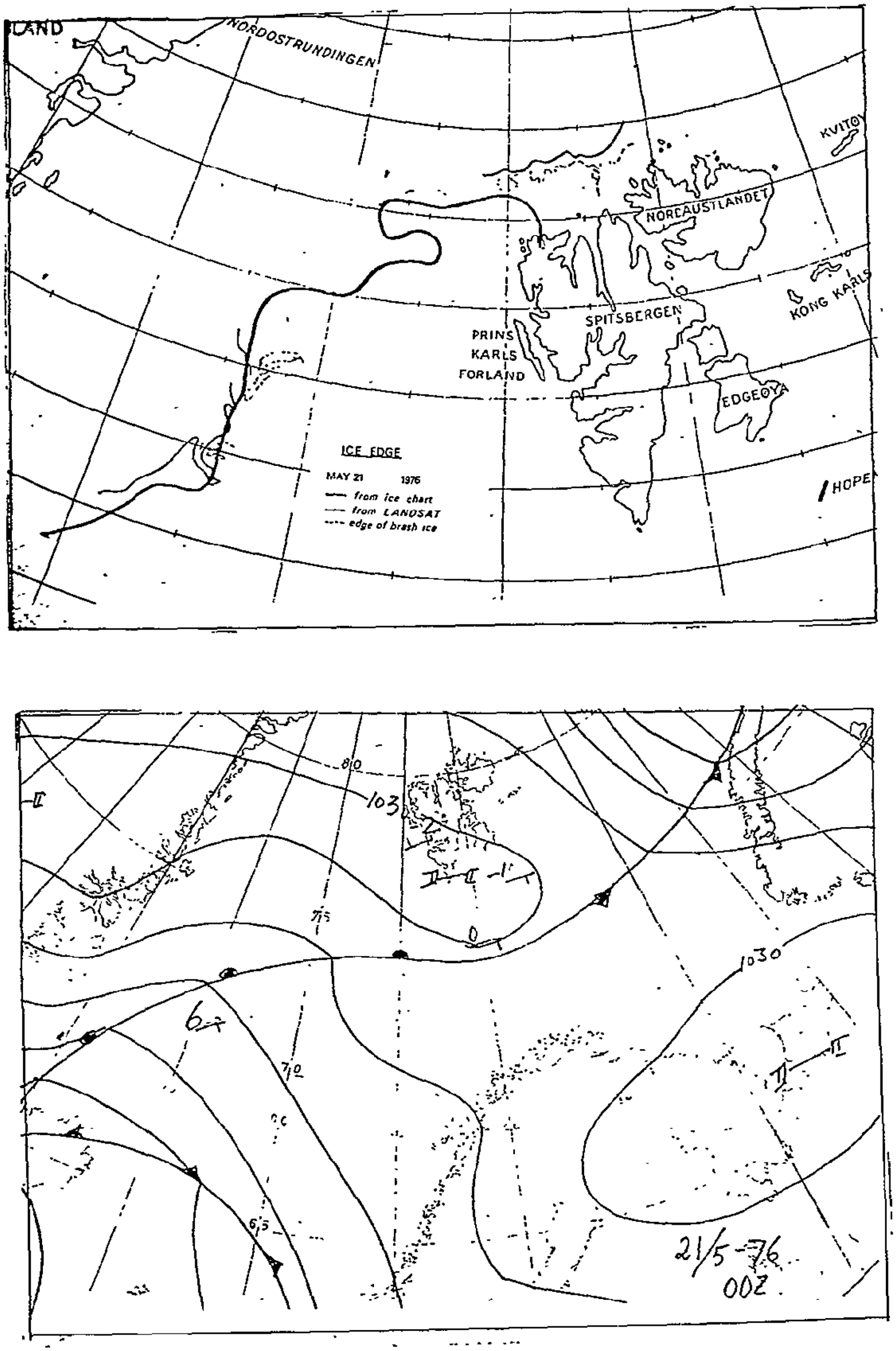


Fig.18

Landsat ice edge compared with ice chart and weather maps 21-22 May 1976.

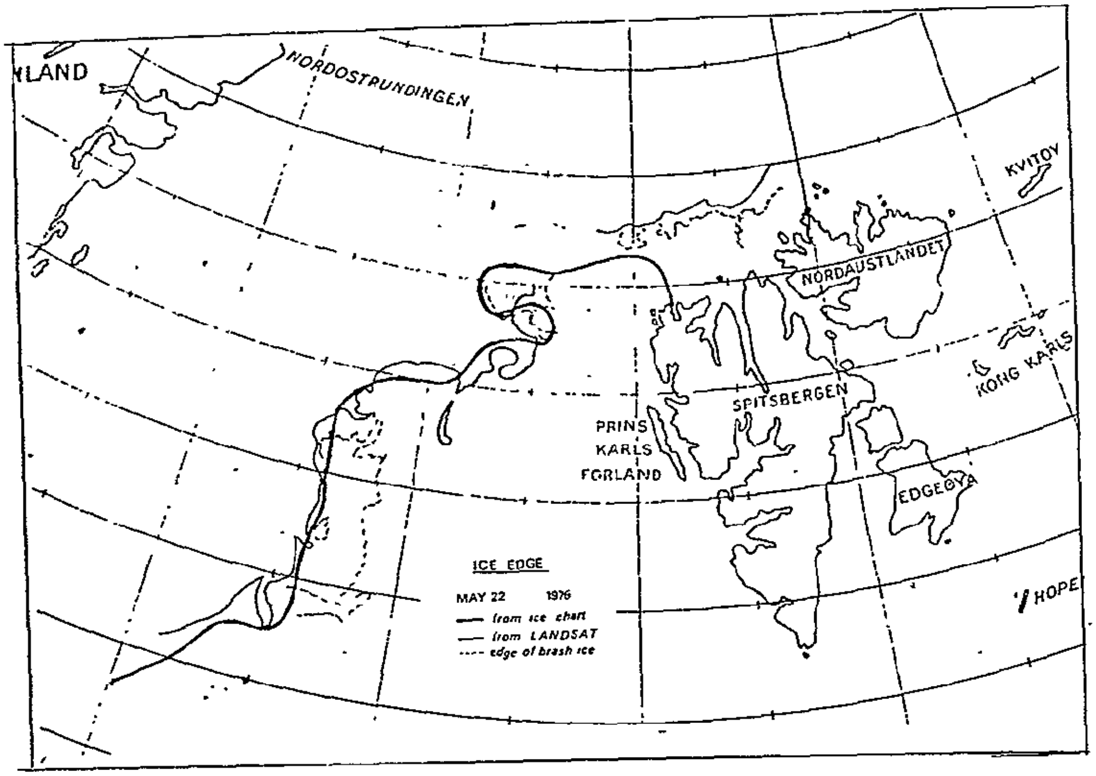

LAND
NORDOSTRUNDINGEN
KVITØY
NORDAUSTLANDET
KONG KARLS
SPITSBERGEN
PRINS KARLS FORLAND
EDGEØYA
HOPE
ICE EDGE
MAY 22 1976
from ice chart
from LANDSAT
edge of brash ice


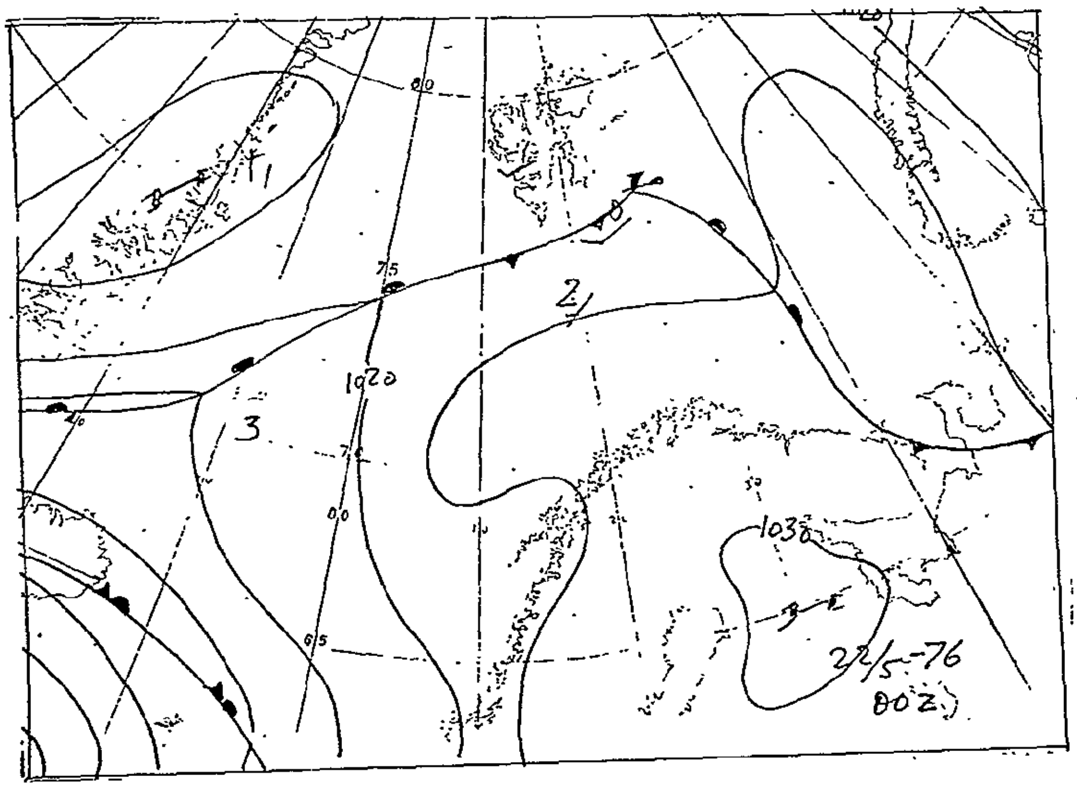

80
75
2
1020
3
70
60
65
1038
22/5-76
00Z


Fig.18 contd.

Fig.18 contd.

Characteristic ice edge during conditions with wind blowing towards the open sea.Cf.Fig.16.

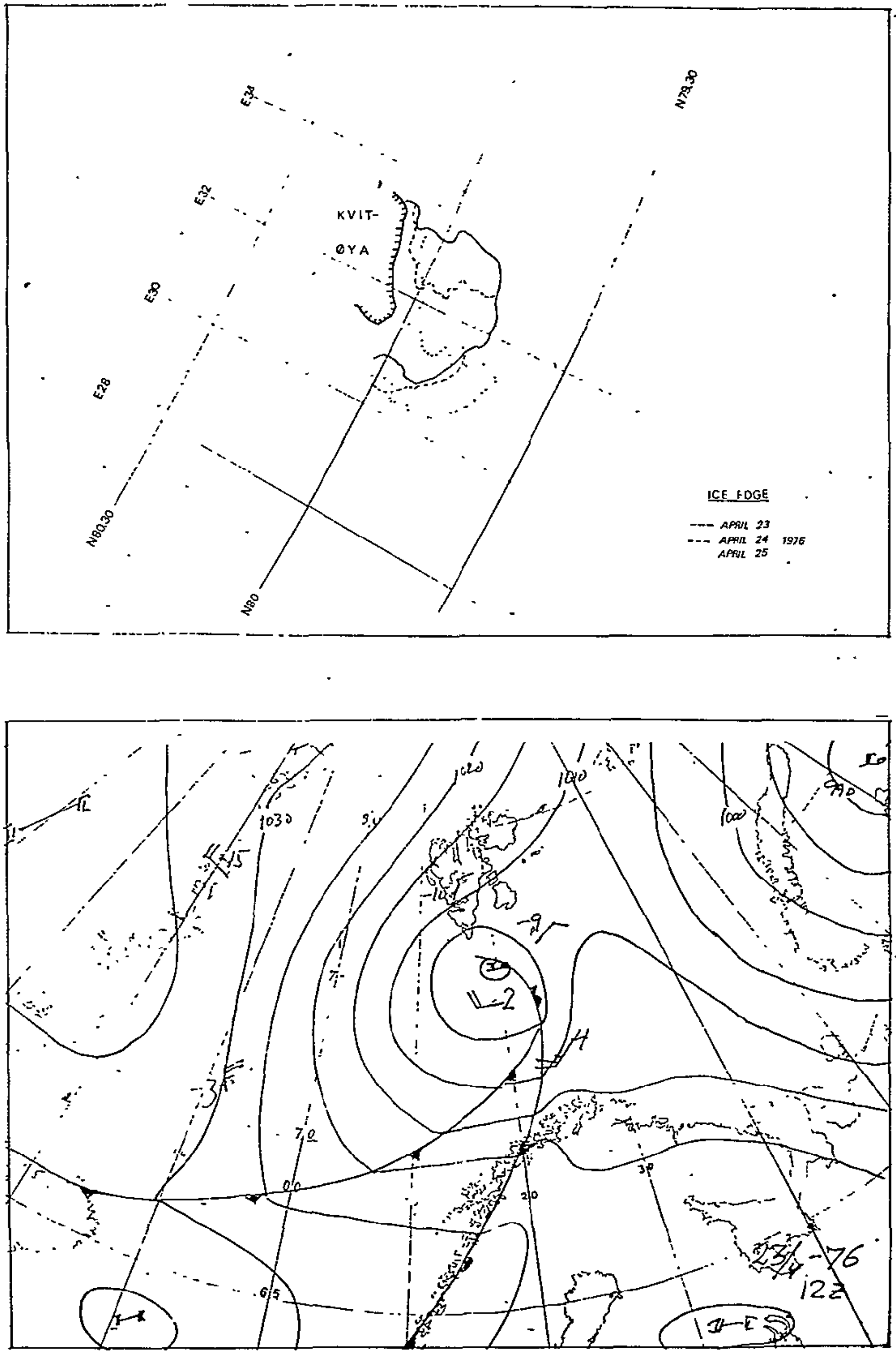


Fig.19

Displacement of ice edge and corresponding weather maps 23-25 April 1976.

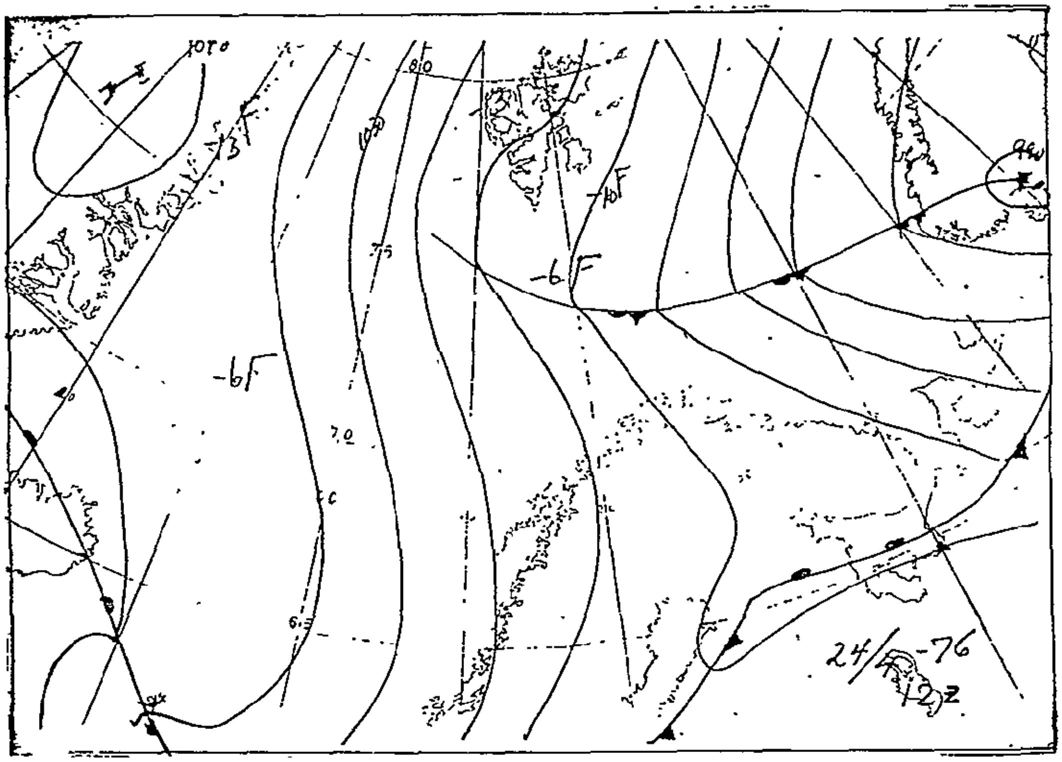


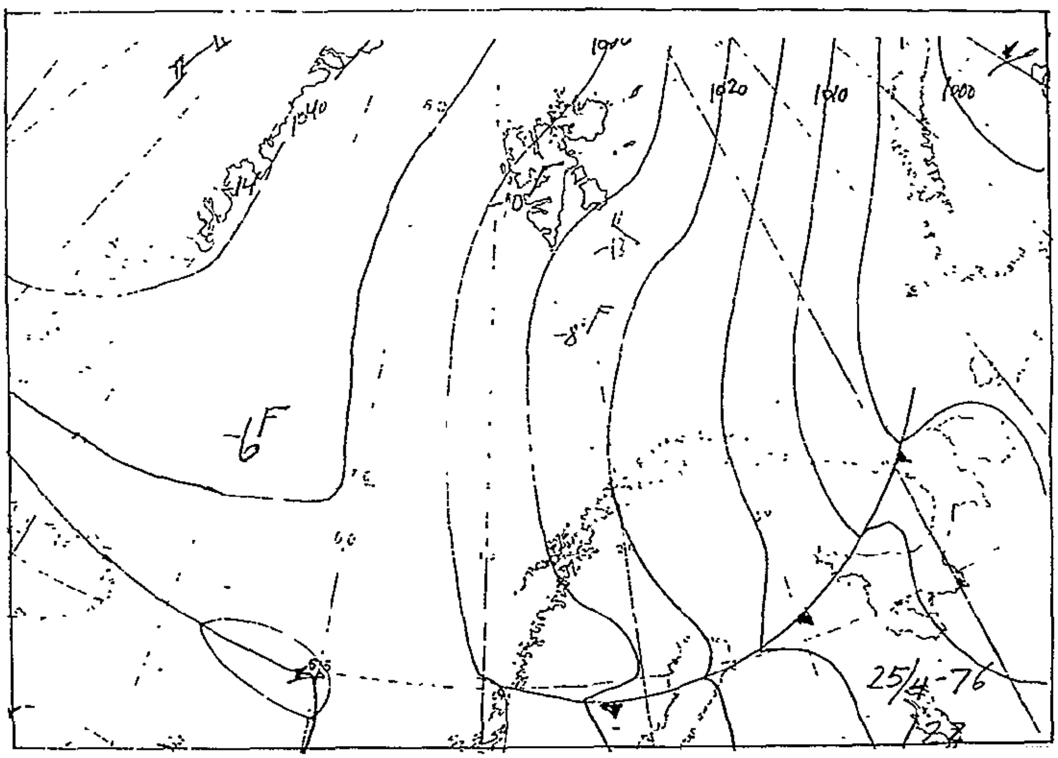


Fig.19 contd.

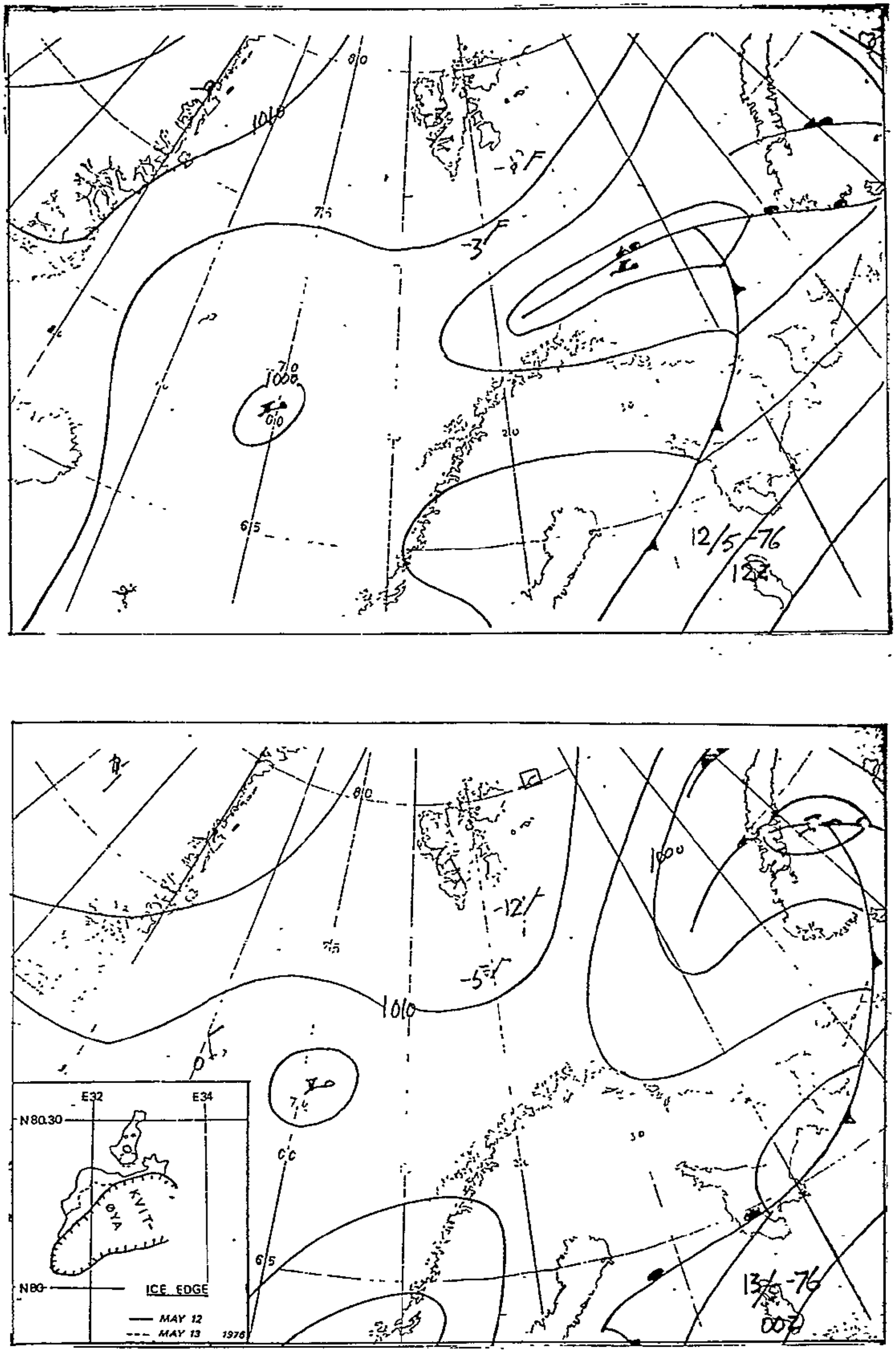


Fig.20

Displacement of ice edge and corresponding weather maps 12-13 May 1976.

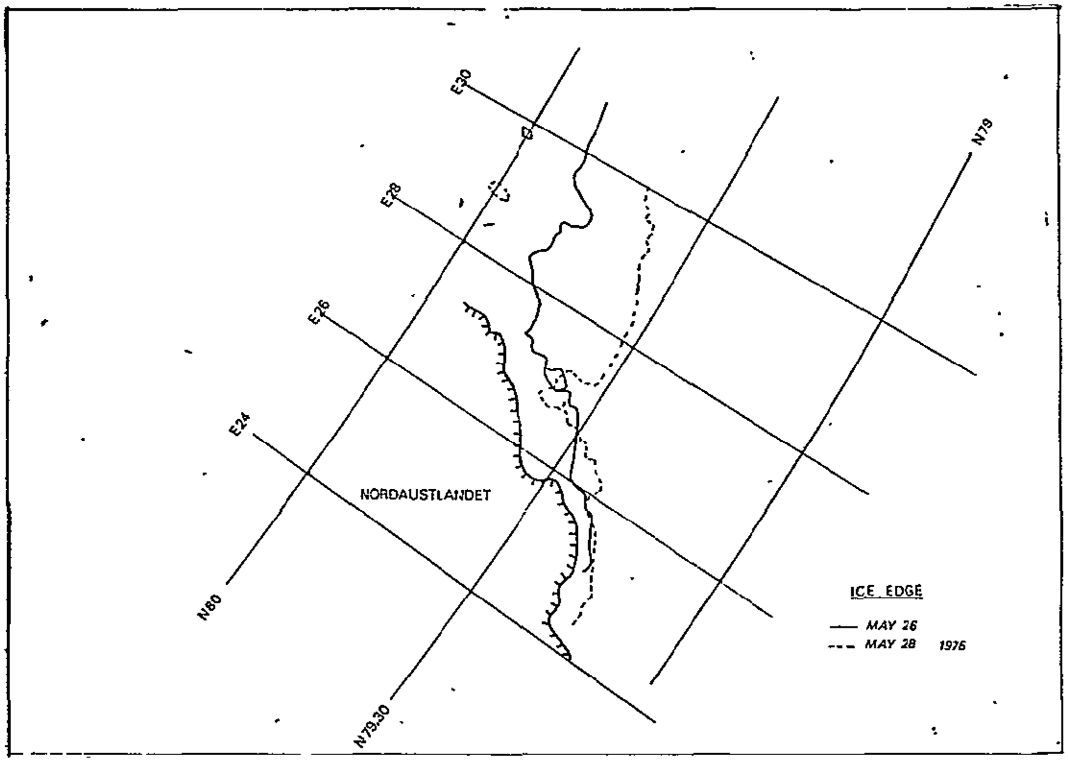


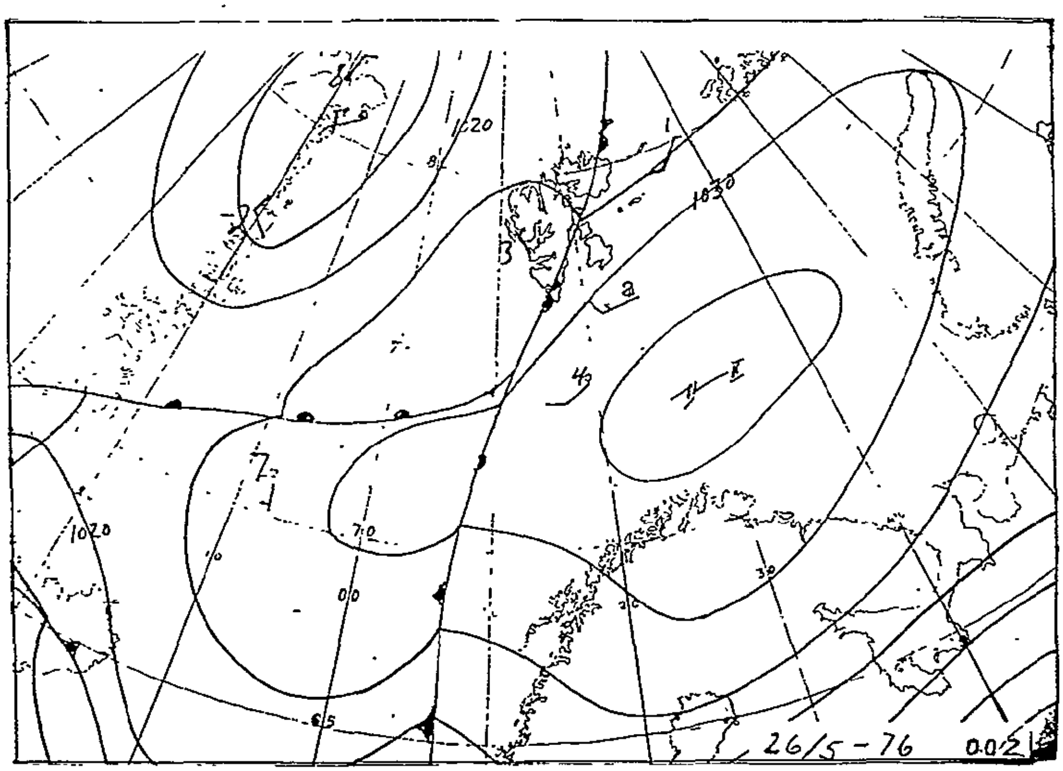


Fig.21

Displacement of ice edge and corresponding weather maps 26-28 May 1976.

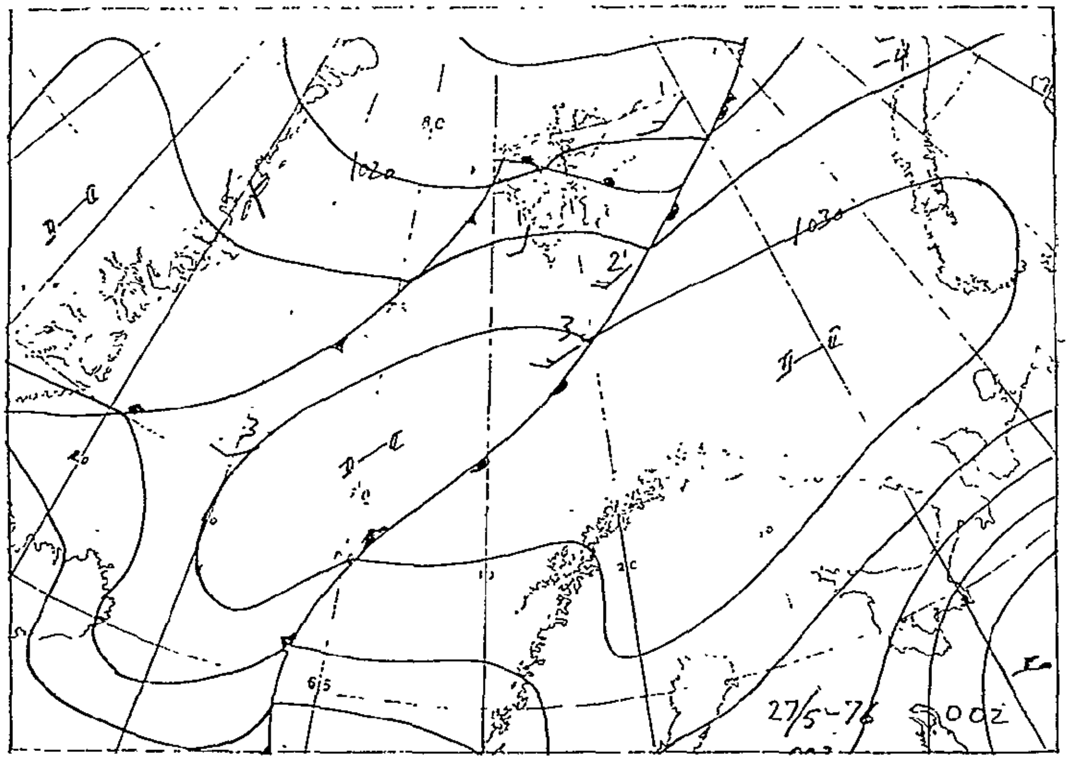


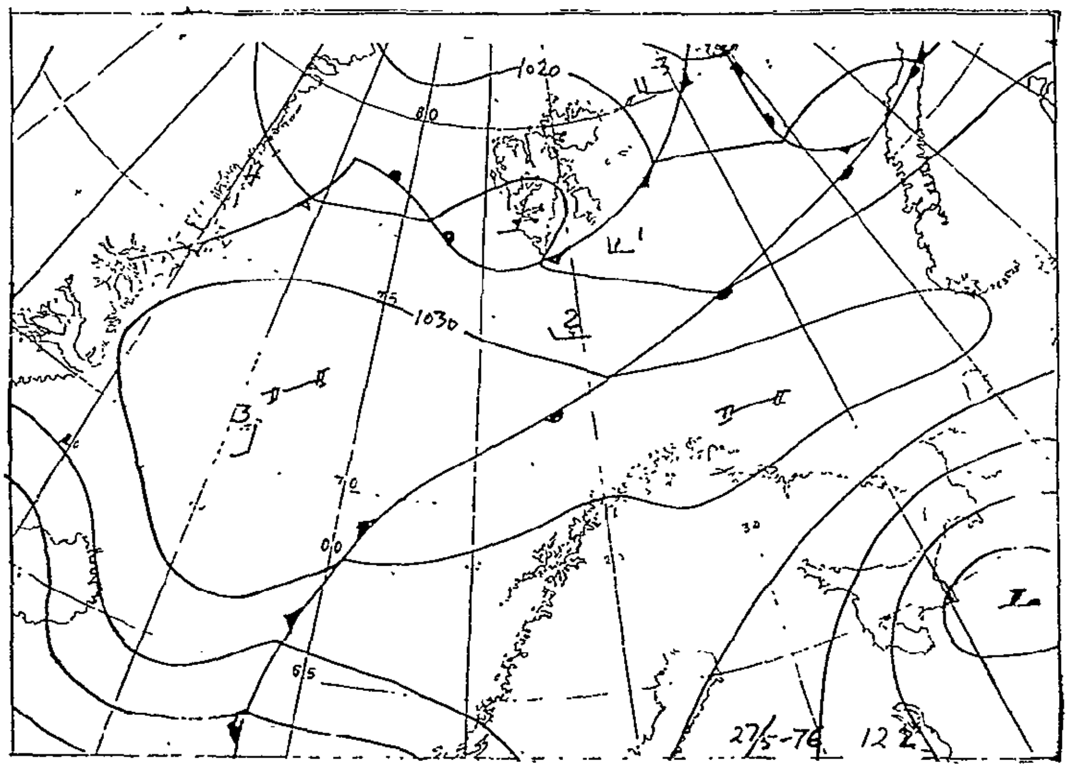


Fig.21 contd.

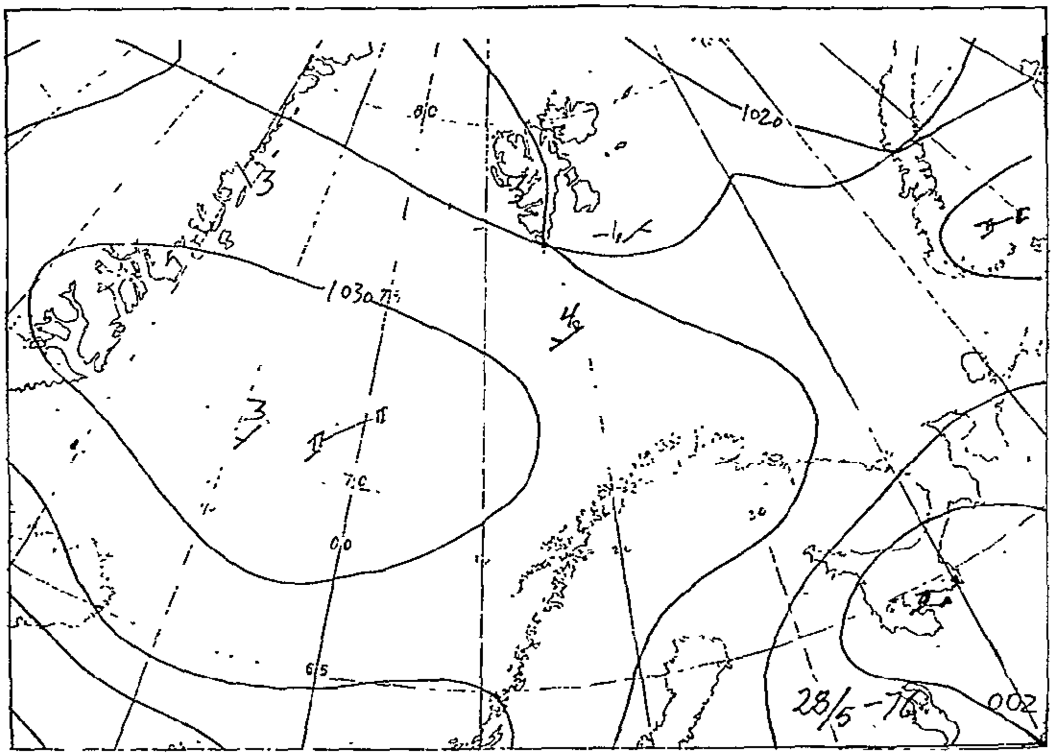


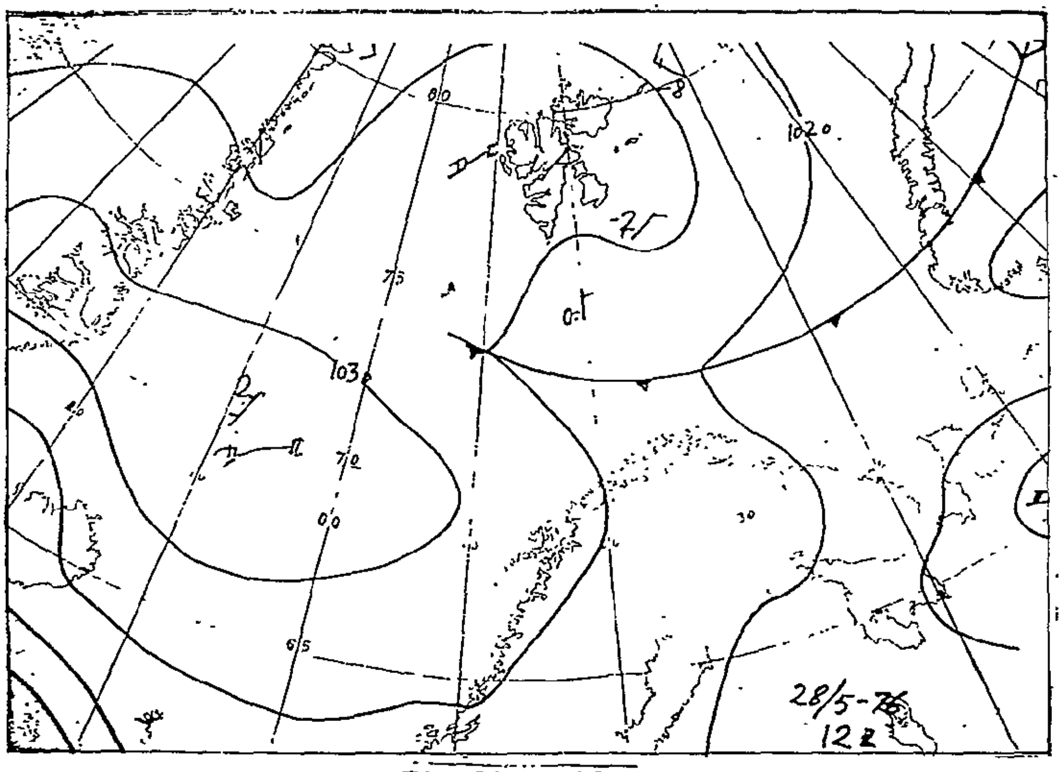


Fig.21 contd.

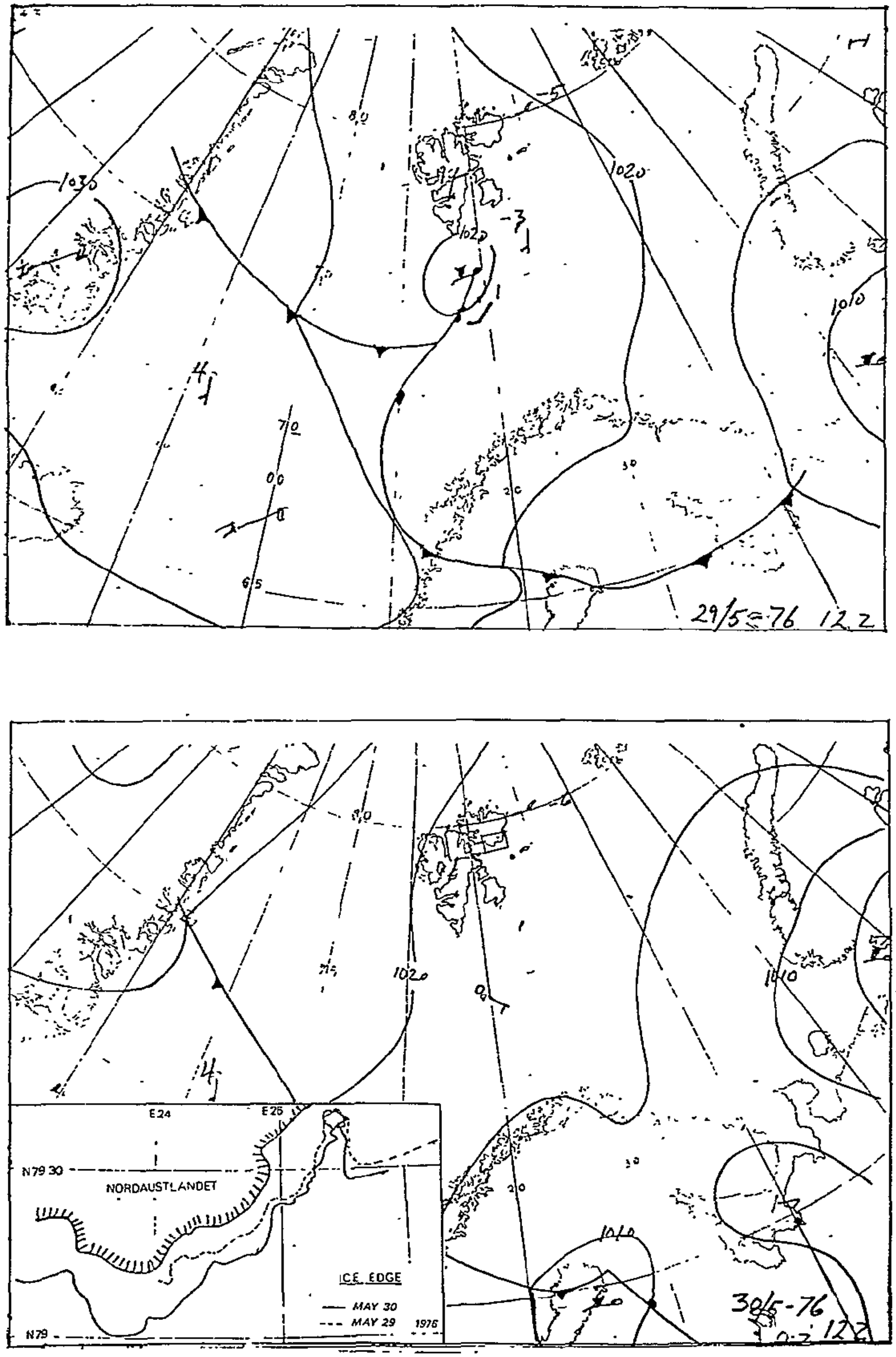


Fig.22

Displacement of ice edge and corresponding weather maps 29-30 May 1976.

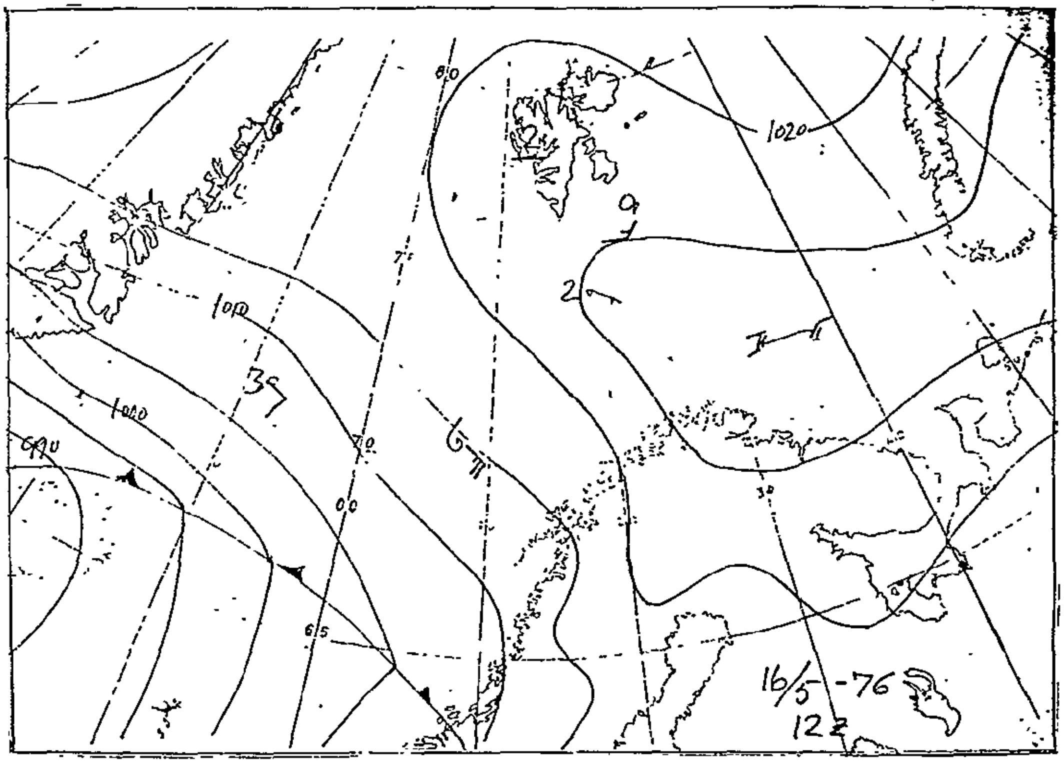


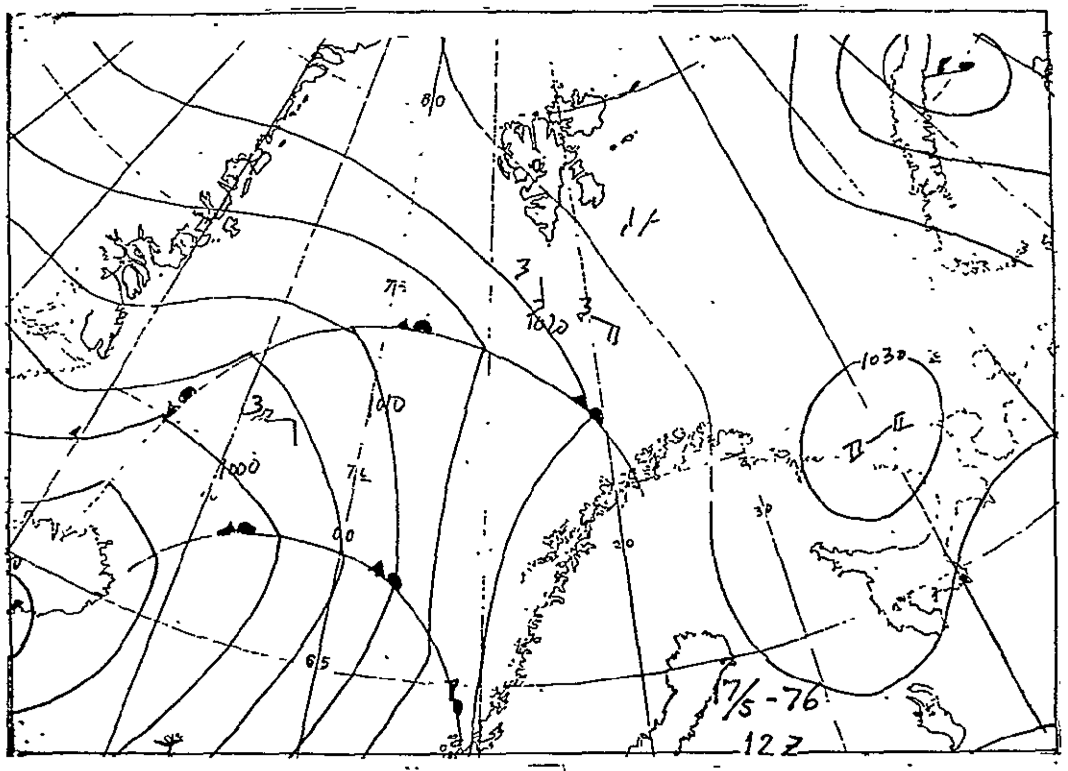


Fig.23

Displacement of ice edge and corresponding weather maps 16-19 May 1976.

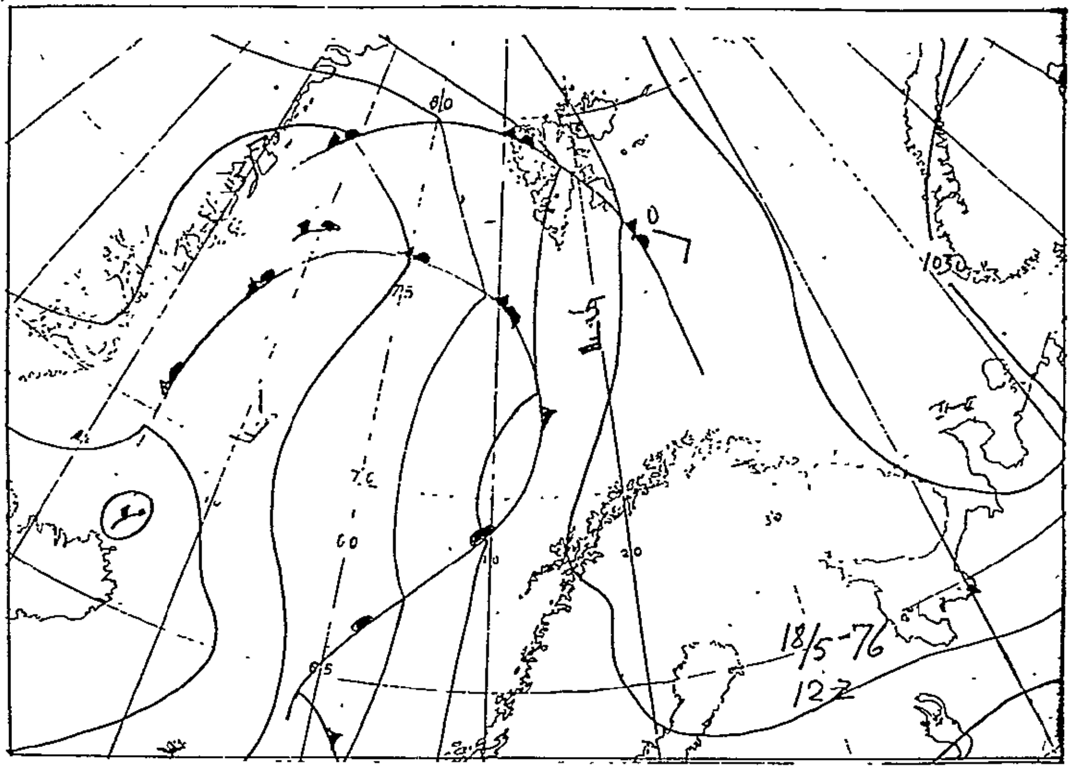
18/5-76
12Z

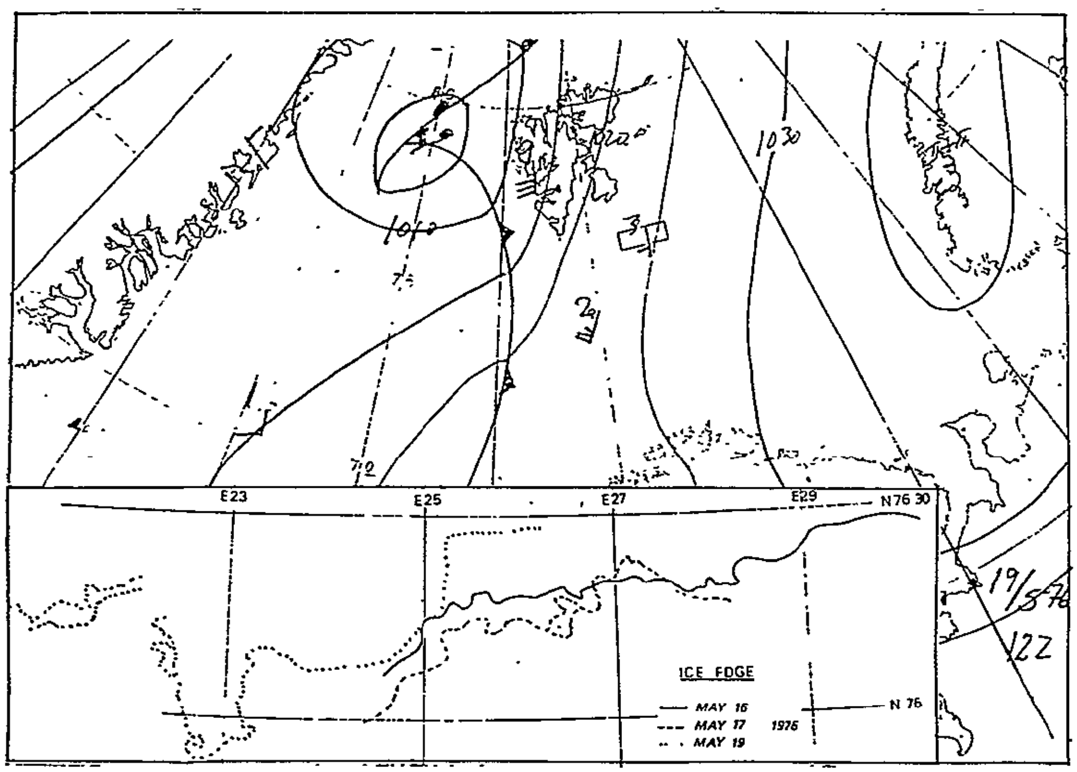
1030
19/5-76
12Z
E23
E25
E27
E29
N76 30
ICE EDGE
MAY 16
MAY 17
1976
MAY 19
N 76

Fig.23 contd.

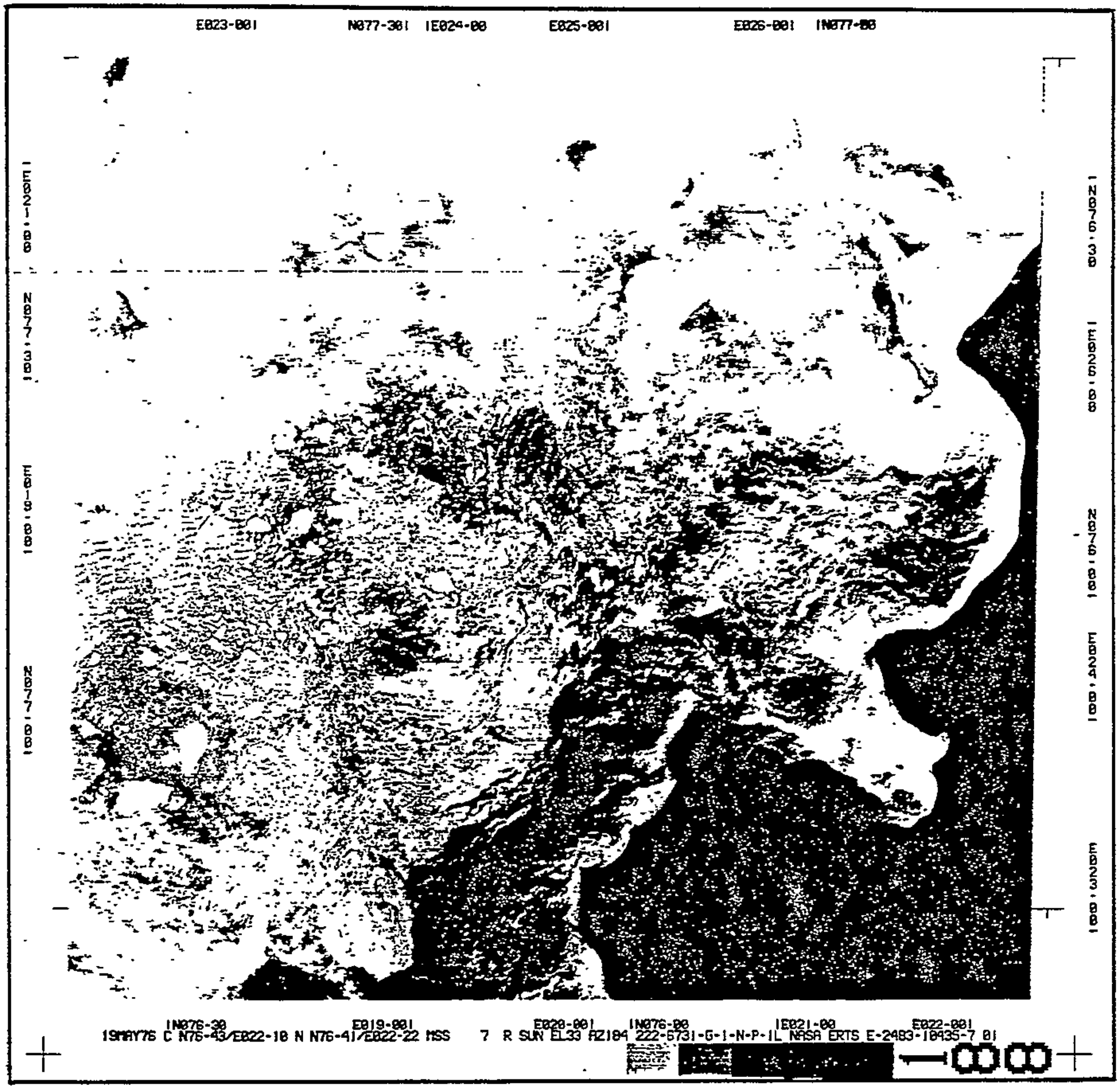

Fig.23 contd.

Characteristic outer ice edge.It is formed when the wind direction after beeing northerly for several days,becomes southerly.